sustainability

MDPI

Article

Sizing Photovoltaic Self-Consumption Systems for Sustainable Decision-Making: A Novel Techno-Economic Approach Using Performance Metrics and Real Consumption Data

Kiane Alves e Silva *, Luis Miguel Carrasco, Rita Hogan Almeida, Luis Narvarte and Eduardo Lorenzo

Instituto de Energía Solar, Universidad Politécnica de Madrid (IES-UPM), 28040 Madrid, Spain; luismiguel.carrasco@upm.es (L.M.C.); rita.hogan@upm.es (R.H.A.); luis.narvarte@upm.es (L.N.); antonio.lorenzo@upm.es (E.L.)

* Correspondence: kiane.asilva@upm.es

Abstract

Photovoltaic (PV) self-consumption systems are increasingly adopted as part of the energy transition, yet residential users often lack the technical background needed to compare alternatives, particularly when storage (ST) is included. To support informed, technically consistent, and sustainable decision-making, this work presents a techno-economic tool for assessing and sizing PV self-consumption systems through hourly energy-balance simulation. Using real consumption, meteorological data, and electricity tariffs, the tool evaluates technical and economic performance and introduces the Mismatch Index (*MI*) to quantify the temporal alignment between PV production and demand. Combined with self-consumption (*SC*) and self-sufficiency (*SS*) metrics, *MI* supports consistent comparison of PV–ST configurations under real operating conditions and helps identify solutions that improve local energy use without unnecessary oversizing. The approach is applied to a residential consumer and to an energy community, comparing individual and centralized solutions. In the residential case, the selected configuration reached a *SC* of 87%, *SS* of 66%, and an *IRR* of 4.92%. For the energy community, the centralized solution increased the 20-year NPV from €1370 for individual systems to €20,060. Analysis of two years of hourly consumption data from 118 households indicated an uncertainty of 10–15% in average hourly consumption when one-year data is used.

Keywords: photovoltaic systems; self-consumption; storage system; sustainable energy use; PV sizing

Check for updates

Academic Editor: John Bell

Received: 4 February 2026
Revised: 10 March 2026
Accepted: 16 March 2026
Published: 18 March 2026

Copyright: © 2026 by the authors. Licensee MDPI, Basel, Switzerland. This article is an open access article distributed under the terms and conditions of the Creative Commons Attribution (CC BY) license.

1. Introduction

The consumption of energy from local photovoltaic (PV) generation, known as PV self-consumption, is an important activity within global energy transition strategies aimed at addressing the energy crisis. Driven by the European Union's (EU) Clean Energy Package [1], passive consumers have become active participants, being able to produce, manage, and store their own electricity, thereby contributing to changes in consumption and production patterns. From the consumer's perspective, these systems reduce dependence on the grid and offer energy security and protection against electricity price fluctuations. They can also lead to savings, since self-generated PV electricity usually costs less than grid electricity. Between 2020 and 2024, the European market incorporated 57.4 GW of PV power in residential self-consumption systems [2], and it is estimated that capacity

additions will continue to increase in the coming years, ranging from 23 to 28 gigawatts per year between 2025 and 2028 [3], reflecting this growing interest.

The rapid expansion of the solar market in Europe has led to a high demand for installation services, resulting in the establishment of a large number of companies in this sector [4]. While this expansion supports EU objectives and contributes to raising awareness of sustainability, end users frequently confront a large volume of competing offers that differ in price, system size, and the addition of a storage unit (ST). Price dispersion reflects heterogeneous costs and business strategies; however, significant discrepancies in system size should not occur when proposals rely on the same inputs, i.e., the same roof tilt angle and orientation, and the same solar irradiation and energy consumption profile.

To support users to understand and compare the performance of different system configurations, technical indicators such as self-consumption (*SC*) and self-sufficiency (*SS*) are particularly useful. Luthander et al. [5] define *SC* as the share of PV energy consumed on site, and *SS* as the proportion of the user's total energy demand covered by the PV system. For end users, these indicators clarify how the system contributes to reducing energy costs and increasing independence from the grid. *SC* is commonly associated with savings by reducing purchases from the grid [6], while *SS* reflects autonomy from the grid. Increasing both indicators increases benefits for the users [7]. Since these indicators depend mainly on solar irradiation and the user's energy consumption profile, which tend to follow consistent and predictable patterns over time, they may offer a consistent basis for evaluating performance and a degree of protection against market uncertainties.

Existing tools for sizing PV self-consumption are commonly based on maximizing one or both indicators. For example, in [8], the authors evaluated ST alternatives to improve *SC* and *SS* in renewable energy applications. In [9] a sizing approach for PV-ST systems has been introduced evaluating how each component influences these metrics. Reference [10] presents a PV size methodology to maximize *SC* comparing two different systems configurations and how the results affect economic evaluation metrics. Similarly, reference [11] reviews methods to increase *SC* in residential seettings, highlighting energy storage and load management. In [12], the authors developed a net-zero factory design approach and used *SC* as a main indicator to assess the effect of PV–ST integration and operational flexibility on local PV utilization. In [13], an integrated PV–ST system with electric vehicles has been evaluated using *SC* and *SS* indicators to quantify the contribution of ST and energy management strategies to on-site renewable use.

Technically, although *SC* and *SS* evaluate system performance, they provide only an indirect assessment of the adequacy of the system relative to user demand because both metrics summarize the amount of overlap energy between PV generation and load overtime, without explicitly characterizing how that overlap is distributed along the time series. Therefore, a metric that directly measures the alignment between energy consumption and PV production provides complementary information. This is relevant because configurations with better temporal correspondence between generation and demand may reduce surplus generation and improve interaction with the grid.

This paper introduces a new metric: the Mismatch Index (*MI*), derived from the Gini Coefficient (*GC*) and Lorenz Curve [14,15], widely used in the statistical analysis of social income inequality. Previous energy studies have adopted GC in conceptually related ways, consistent with the argument of [16] that Lorenz-based measures are not specific to income and can be applied to any non-negative size distribution to quantify inequality (or unevenness) across a set of observations. For instance, ref. [17] used "energy Lorenz curves" and Gini coefficients to describe distribution and equity in electricity consumption across populations, rather than temporal PV–load coincidence. In the PV domain, ref. [18] proposed a Lorenz-based approach to quantify variability/concentration

of PV power output itself, without requiring a load time series. More directly related to PV–load matching, ref. [19] quantified mismatch between PV generation and typical load patterns, where GC is applied after a data-driven extraction of representative demand profiles, and the results are interpreted at the level of load-pattern classes. In contrast, the *MI* proposed here is formulated to assess the degree of temporal alignment between PV generation and electricity demand at the system (or user) level, and it can be computed directly from the PV–load balance time series used in self-consumption assessment.

Here, the approach has been adapted to assess the mismatch between energy output from the PV systems (including storage discharge when present) and electricity demand in the context of self-consumption. In related PV–load applications, GC is commonly defined on PV generation and demand time series (or on PV output variability), whereas here storage discharge is explicitly included in the supply term when available. Given the common mismatch between PV generation and demand, *MI* complements *SC* and *SS* by providing a more complete characterization by jointly describing (i) the magnitude of PV–load overlap (*SC* and *SS*) and (ii) the degree of temporal alignment between both distributions over the year. This combination supports a more granular comparison of self-consumption system configurations, particularly when distinguishing between technically similar solutions with different levels of demand-oriented matching.

Although *SC*, *SS* and *MI* support technical assessment, end user decisions are usually based on cost and profitability. Therefore, economic feasibility analysis often complements the technical evaluation to support investment optimization [20], compare design options under consistent economic criteria [21], and avoid economically disadvantageous systems configurations [22]. Common metrics include the Payback Period (*PBP*) and the Internal Rate of Return (*IRR*) [23], with Levelized Cost of Energy (*LCOE*) frequently applied [24]. The *PBP* indicates the time required to users recover their initial investment, *IRR* signals whether expected returns justify the investment, and *LCOE* benchmarks the energy unit cost (€/kWh) from the PV system against grid electricity tariffs, offering a fixed and transparent cost in contrast to uncertain and fluctuating grid prices. In addition, this work includes the Levelized Profit of Energy (*LPOE*), which measures the net revenue per kWh of electricity from solar PV generation, introduced by [25] as an analogue and supplement to *LCOE*.

Numerous sizing tools have emerged over time to address the rapidly growing market for PV self-consumption. Kazem et al. (2022) presents a systematic review spanning eight decades, cataloguing 36 tools that may focus on system sizing, performance, and cost evaluation [26]. Representative examples of widely used tools and frameworks for PV and PV–ST assessment include PVsyst [27], HOMER Pro [28], and NREL SAM [29]. Appendix A summarizes these tools and highlights their data resolution, accessibility, and whether an explicit temporal matching criterion is used in the sizing logic. Most tools perform parametric analysis, comparing the results from different systems configurations, while a smaller group performs system optimization that usually minimizes costs under technical constraints. Their methodology relies mostly on monthly or annual aggregated data of weather and load profile. As design criteria, choices balance cost goals with technical needs, returning energy production, self-consumption rate, and cost metrics as common outputs. Other approaches suggest models based on minimizing life cycle cost to identify the most cost-effective technological design in energy communities, using energy demand simulations [22]. In contrast to conventional techno-economic sizing tools, which typically return a single solution for a predefined objective (e.g., cost minimization), this work provides a flexible framework to assess PV–ST configurations through hourly simulation. The tool enables the analysis of how different configurations affect technical, temporal-alignment, and economic indicators, as well as the identification of configurations that satisfy user-defined performance criteria. In addition, it incorporates a rule-based

sizing procedure that evaluates multiple criteria to recommend a single configuration when needed, without relying on mathematical optimization; however, this is only one of its possible functionalities and does not define the framework as a single-solution optimization approach.

Yet, three gaps remain weakly addressed. (i) Many tools, including established commercial software, perform planned energy and load-balance simulations and report overlap-based indicators such as *SC* and *SS*, together with grid interaction metrics. However, an explicit temporal mismatch characterization criterion is less commonly used as a primary sizing objective for grid-connected PV self-consumption systems. In particular, sizing workflows typically optimize energy or cost metrics, while the structure of mismatch across time steps is either assessed qualitatively or treated indirectly. (ii) Design tools often rely on monthly or yearly aggregated demand instead of annual hourly data; as a result, the energy balance becomes imprecise, which can bias self-consumption estimates and lead to incorrect sizing of the PV–ST system. (iii) Few tools qualify as commercial solutions with free access, which limits practical use and independent comparison. In addition, even among freely accessible and reproducible solutions, temporal matching is rarely integrated as an explicit, metric-driven sizing criterion.

Based on these gaps, this study addresses the following research questions:

RQ1: How can temporal mismatch between PV generation and demand be quantified and incorporated into sizing decisions?

RQ2: How technical, temporal, and economic indicators can be integrated within a single decision-support framework?

RQ3: How does the proposed tool performs when applied to residential and energy-community case studies?

To fill these gaps, address these research questions, and address user needs and support informed decisions, this paper presents an open-source tool for sizing PV self-consumption systems and evaluating their technical and economic performance. Using real historical hourly energy consumption profiles and meteorological data, the tool, developed in Python 3.12.1 [30], simulates energy flows and performs both technical and economic analyses with the previously presented indicators. The tool generates graphical outputs that map performance over different PV and ST sizes, including configurations with and without ST. In this way, users can better understand how different system sizes affect technical performance and economic outcomes. To illustrate its functionality, the tool has been applied in two different contexts: (i) an individual residential consumer, to show how the tool assesses PV-ST configurations in terms of mismatch reduction, stabilization of technical performance indicators (*SC* and *SS*) without oversizing, and economic viability criteria, while sizing a PV-ST system that meets these criteria; and (ii) an energy community operating in a village in a rural area in northern Spain [31], with ten prosumers, to compare individual and centralized system solutions based on technical and economic indicators.

Although the case studies rely on residential data, the workflow extends to any context with a defined load profile and demand, such as industrial and commercial consumers.

Finally, the document raises questions about the representativeness of the initial data when using it to size PV systems for self-consumption. Although tools such as PVGIS [32] can generate hourly solar radiation and ambient temperature data for a given geographical location from data series spanning 16 years or more, the availability of electricity consumption data is often limited. In most cases, only monthly consumption bills are available, which makes it impossible to perform an hourly analysis. Electricity distribution companies retain historical consumption data, but only the holder of the consumption point can access it. Permission from the holder is required to consult the data. The authors have had access to two full years (2023–2024) of hourly consumption data from

118 supply points in the Calatayud region in northern Spain, where the aforementioned energy community operates. The data were retrieved from the distribution-company metering system through the open access platform Datadis [33], with explicit authorization granted by the supply-point owners. The sample includes residential and small commercial consumers, predominantly in single-family rural houses. A statistical analysis is presented to compare consumption profiles between the two years of data, quantify interannual variability and establish whether a single year of hourly electricity consumption data could be representative for sizing a PV system for self-consumption.

Therefore, the scientific contributions of this work are threefold. First, it introduces the *MI* to quantify the degree of temporal alignment between PV system energy output and electricity demand in self-consumption applications. Second, it proposes a sizing and assessment framework that combines *MI*, *SC* and *SS* with techno-economic metrics to enable consistent comparison of PV–ST configurations under hourly energy balance. This framework contributes to sustainability-oriented system design by supporting configurations that are more closely aligned with demand, reducing unnecessary surplus, and promoting more efficient interaction with the grid. Third, it provides an empirical analysis of interannual variability in hourly consumption data and its implications for the representativeness of one-year datasets in sizing studies.

The remainder of this paper is organized as follows: the Introduction proceeds with a literature-based overview of PV self-consumption systems and the common technical and economic performance metrics. Section 2 presents the tool description and methodology of each tool's application. Section 3 applies the tool in a case study showing all its functionalities. Section 4 reports comparative results for the energy community analysis. Section 5 presents a statistical comparative analysis of the hourly electricity consumption of 118 residential consumers over two consecutive years. Finally, Section 6 outlines the key conclusions.

1.1. PV Self-Consumption System Overview

In a PV self-consumption system with ST, AC coupling often becomes the preferred option because it offers greater flexibility in system configuration and retrofit integration [8], as illustrated in Figure 1.

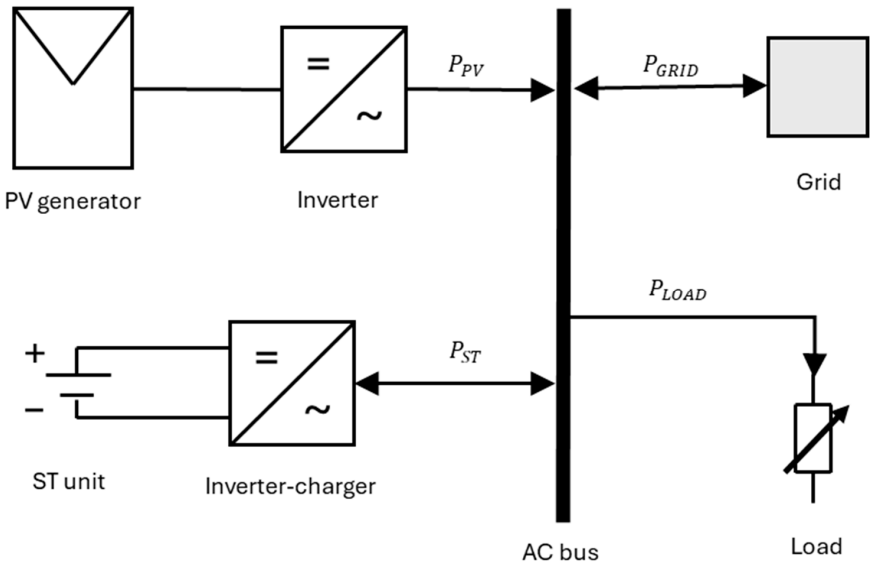


Figure 1. Schematic illustration of the AC-coupled PV self-consumption system with ST considered in this work, showing the PV generator, inverter, inverter–charger, ST unit, load, and grid interface. Arrows indicate the power flow directions used in the hourly energy-balance model.

The main components of the system include the PV generator, the battery (ST), the load demand, and the distribution grid. Equation (1) describes the system's power balance, where the instantaneous power generated by the PV (P_{PV}) equals the sum of the power demanded by the load (P_{Load}), the power exchanged with the grid (P_{Grid}), and the power exchanged with the ST (P_{ST}). Here, P_{Grid} and P_{ST} are considered negative when they supply power to the load, and positive when they absorb surplus power from the PV generator.

$$P_{PV} = P_{Load} + P_{Grid} + P_{ST} \tag{1}$$

PV production can be estimated based on cell temperature (T_C), Nominal Operating Cell Temperature ($NOCT$), effective plane-of-array irradiance (G), and ambient temperature (T_a), as expressed by Equations (2) and (3) [9].

$$T_C = T_a + \left(\frac{NOCT - 20}{800}\right) \cdot G \tag{2}$$

$$P_{PV} = P_{PV}^{*} \cdot \frac{G}{G^{*}} \cdot [1 + \gamma(T_C - T_C^{*})] \cdot \eta \tag{3}$$

where P_{PV}^{*} refers to the PV nominal power, G^{*} refers to the reference solar irradiance, γ is the temperature coefficient of power, and η represents the overall balance-of-system efficiency (including angular, spectral, soiling, mismatch and shading losses as well as inverter and wiring losses).

In self-consumption systems, ST, typically electrochemical battery, contributes to improve *SC* and *SS* by absorbing surplus power from the PV generator. This charging process redirects available power to the ST instead of exporting it to the grid, enabling later power supply to the load during periods of low solar generation or increased demand. By doing so, the system increases the use of locally generated power and reduces dependence on the grid. The state of charge (SOC) determines the ST's ability to absorb or deliver power at any given time, directly influencing how the system manages power flows.

1.2. Self-Consumption and Self-Sufficiency Indicators

Under PV self-consumption system configuration, Luthander et al. [5] describe the instantaneous self-consumption power ($M(t)$) as the minimum between the load demand and the total power available from the PV generator and the ST, as expressed in Equation (4). The equation shows that the self-consumption power is limited by whichever of the load and generation profiles is smaller at any given time.

$$M(t) = min\{P_{Load}(t), P_{PV}(t) + P_{ST}(t)\} \tag{4}$$

Note that $P_{ST}(t) < 0$ when charging the battery and $P_{ST}(t) > 0$ when discharging.

The *SC* and *SS* metrics can be expressed by Equations (5) and (6), respectively, as described in [10]. In these equations, integrals represent the calculations based on the instantaneous power balance over time, while the second part relates to the energy balance of the system. Since E_X^Y represents the energy flow from origin X to destination Y, E_{PV}^{Load} and E_{ST}^{Load} refer to the energy supplied to the load by the PV generator and the ST, respectively. E_{PV} is the total amount of PV energy generated over a one-year period, while E_{Load} is the total load demand over the same one-year period.

$$SC = \frac{\int_{t_1}^{t_2} M(t)dt}{\int_{t_1}^{t_2} P_{PV}(t)dt} = \frac{E_{PV}^{Load} + E_{ST}^{Load}}{E_{PV}} \tag{5}$$

$$SS = \frac{\int_{t_1}^{t_2} M(t)dt}{\int_{t_1}^{t_2} P_{Load}(t)dt} = \frac{E_{PV}^{Load} + E_{ST}^{Load}}{E_{Load}} \quad (6)$$

Other relevant metrics for on-grid systems are related to grid interaction [5] and are based on the energy imported from (IE) and exported to (EE) the grid, as described in Equations (7) and (8), respectively. IE is defined as the portion of energy demand that must be supplied by the grid (E_{Grid}^{Load}) when the self-consumption system cannot fully cover consumption, while EE refers to the surplus energy that exceeds on-site consumption and ST capacity, resulting in its export to the grid (E_{PV}^{Grid}).

$$IE = \frac{E_{Grid}^{Load}}{E_{Load}} \quad (7)$$

$$EE = \frac{E_{PV}^{Grid}}{E_{PV}} \quad (8)$$

1.3. Economic Evaluation Metrics

From an economic perspective, power flows determine the system revenues (savings from self-consumption and income from surplus electricity sales), directly influencing the economic viability indicators. The PBP represents the time required for the accumulated revenues to match the initial investment (I_0). In its simplest form, it can be expressed in Equation (9) [11].

$$PBP = \frac{I_0}{REV - C} \quad (9)$$

where REV corresponds to the annual revenue and C expresses the annual operating cost.

The IRR represents the annualized rate of return generated by the investment. Its definition builds on the Net Present Value (NPV), which measures the difference between the present value of future profits and the initial investment, considering the time value of money over the system lifetime (LT), as expressed in Equation (10). The IRR corresponds to the discount rate (r) that results in a zero NPV, as defined in Equation (11) [34].

$$NPV = -I_0 + \sum_{t=1}^{LT} \frac{REV_t - C_t}{(1+r)^t} \quad (10)$$

$$IRR = r \ : NPV = 0 \quad (11)$$

The $LCOE$ estimates the average cost per kilowatt-hour (kWh) of electricity produced over the system's lifetime, considering the annual PV degradation rate (d_{PV}), calculated as the ratio of total discounted costs to total generated energy [34], as expressed in Equation (12).

$$LCOE = \frac{I_0 + \sum_{t=1}^{LT} \frac{C_t}{(1+r)^t}}{\sum_{t=1}^{LT} E_{PV}(1-d_{PV})^{t-1}} \quad (12)$$

While $LCOE$ condenses the unit cost of produced energy, $LPOE$ [25] also considers the REV, thereby complementing $LCOE$. It measures the net profit per kWh, as defined by Equation (13). When used jointly, $LCOE$ guides cost efficiency, and $LPOE$ frames market-facing feasibility and grid-parity appraisal for self-consumption systems.

$$LPOE = \frac{NPV}{\sum_{t=1}^{LT} E_{PV}(1-d_{PV})^{t-1}} \quad (13)$$

2. Tool Description and Methodology

Four individual applications compose the tool: (i) Energy Flow Application (EFA); (ii) Consumption–Generation Alignment Application (CGA); (iii) Economic Assessment Application (EAA); and (iv) System Sizing Application (SSA). Figure 2 summarizes the overall workflow of the tool.

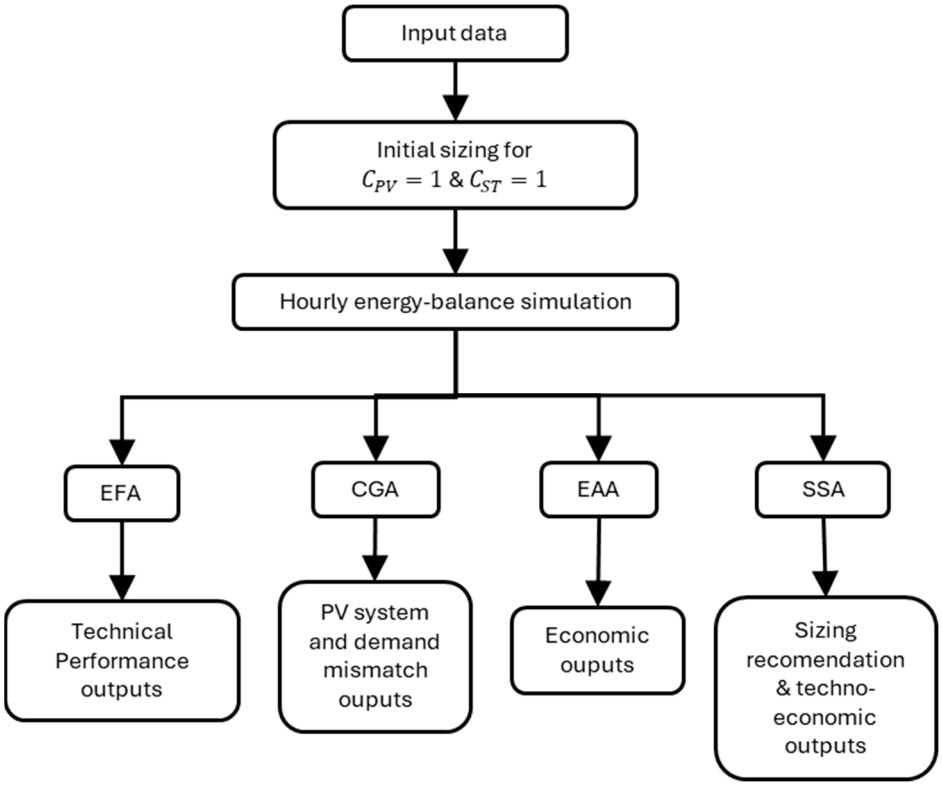


Figure 2. Overview of the tool structure. The tool uses input data and hourly energy-balance simulations to generate outputs through four applications: Energy Flow Analysis (EFA) for technical performance, Consumption–Generation Alignment (CGA) for mismatch characterization using the Mismatch Index (*MI*), Economic Assessment Application (EAA) for economic indicators, and System Sizing Application (SSA) for the final sizing recommendation and the corresponding techno-economic results.

As common ground, all applications have been developed based on an hourly energy-balance simulation. To run it, the tool requires as input one year of actual hourly data on energy consumption, irradiance, and ambient temperature. This common modelling basis also supports the identification of configurations that better use locally generated electricity under actual consumption conditions.

To compare system configurations consistently, the analysis applies two normalized sizing parameters: PV Capacity (C_{PV}) and ST Capacity (C_{ST}). The first refers to the annual ratio between total PV generation (E_{PV}) and demand (E_{Load}) over a year, as defined in Equation (14). The second represents the ratio of the ST capacity (E_{ST}) to average daily consumption, calculated by dividing the annual load by the number of days in a year (n_y), as expressed in Equation (15). Although they are expressed as "capacities" for brevity, both parameters are energy-based normalizations and can be translated into practical sizes (kWp and kWh) using the PV nominal power (kWp) and ST energy capacity (kWh).

$$C_{PV} = \frac{E_{PV}}{E_{Load}} \quad (14)$$

$$C_{ST} = E_{ST} \times \frac{n_y}{E_{Load}} \quad (15)$$

As a practical example, if a $P_n = 3$ kWp is needed to meet the annual demand ($E_{PV} = E_{Load}$) in the reference case ($C_{PV} = 1$), then $C_{PV} = 0.5$ corresponds to $P_n = 1.5$ kWp and $E_{PV} = 0.5 \times E_{Load}$ under the same conditions. Likewise, if the average daily consumption is 10 kWh/day, then $C_{ST} = 0.5$ corresponds to a ST capacity $E_{ST} = 5$ kWh.

For methodological delimitation, the parameter interval has been defined as $C_{PV} \in [0,\ 1.5]$ and $C_{ST} \in [0,\ 1]$, both with a step size of 0.01. The following subsections present the methodological criteria for each application.

As an initial sizing step, a reference configuration is defined at $C_{PV} = 1$ and $C_{ST} = 1$, which corresponds to (i) annual PV generation matching annual demand and (ii) storage energy capacity matching average daily consumption. This reference case is used to scale the PV generation profile and storage capacity for any (C_{PV}, C_{ST}) pair. The hourly energy-balance simulation is then executed for each configuration in the sizing space, generating annual energy-flow outputs that serve as the common basis for EFA, CGA, EAA, and SSA.

Building on the PV self-consumption architecture in Section 1.1, Figure 3 summarizes the operating logic sequence of the energy-balance simulation tool:

1. At each hour (t) PV energy first supplies the load.
2. If PV exceeds the load:
3. Any surplus goes to charge the ST subject to state of charge (SOC) bounds.
4. With SOC at 1, any remaining surplus exports to the grid.
5. If PV does not cover the load:
6. Discharge the ST.
7. If SOC is zero and the load remains unmet, import the remainder from the grid.

Note that, in this proposed energy flow scheme, the grid cannot charge the ST.

2.1. Energy Flow Application (EFA)

The EFA examines how system size influences technical performance, in terms of *SC*, *SS*, *IE*, and *EE*, focusing on energy interactions. For each PV–ST configuration over the above-defined parameter interval, the tool computes the hourly energy balance and then derives the indicators from flows between PV, the ST, the load, and the grid, computed hour by hour and then summed over a full year [35].

To avoid oversizing, EFA applies a stabilization criterion. As the algorithm scans the parameter interval, each step updates the indicators; once changes in *SC* and *SS* indicators stay within a tolerance ($\tau = 1\%$), the configuration counts as stabilized. For example, when increasing the battery size leads to an increase in *SC* of less than 1%, the stabilization point is considered reached. This point defines the chosen battery size (C_{ST}).

As an outcome, EFA provides three complementary views:

- Energy-flow plots that sweep one sizing parameter while holding the other fixed, displaying *SC*, *SS*, *IE*, and *EE* on the same axes for direct comparison.
- 3D surfaces that map each indicator over the (C_{PV}, C_{ST}) space to reveal global trends.
- Iso-curves that identify (C_{PV}, C_{ST}) combinations delivering the same indicator value, useful for target-driven sizing.

2.2. Consumption–Generation Alignment Application (CGA)

2.2.1. MI Definition and Implementation in CGA

The CGA quantitatively evaluates the alignment between system energy output (*SEO*) and energy consumption distributions over time using the Mismatch Index (*MI*), using the full 8760 hourly values from the annual energy balance. The *MI* calculation procedure is detailed below.

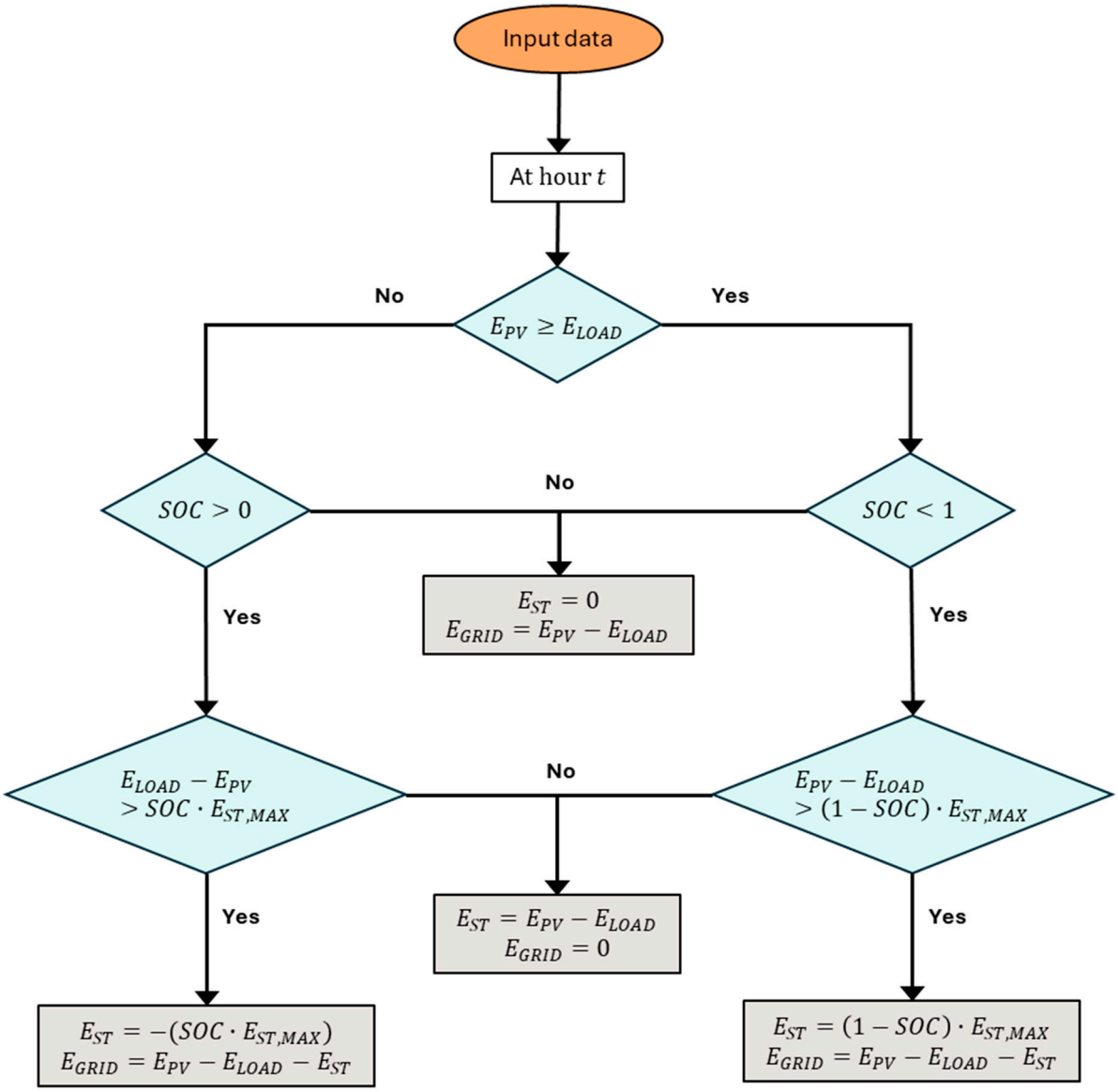


Figure 3. Hourly energy-balance dispatch logic implemented in the tool. At each timestep PV generation supplies the load first; surplus energy charges the ST and remaining energy is exported. If PV is insufficient, the ST discharges and any unmet load is imported.

For a given (C_{PV}, C_{ST}) configuration, CGA computes *SEO* from the one-year hourly energy balance, as in Equation (16). *SEO* represents the total energy delivered by the PV system, including ST discharge.

$$SEO = E_{PV}^{Load} + E_{PV}^{Grid} + E_{ST}^{Load} \tag{16}$$

where E_{PV}^{Load} refers to the PV energy used directly by the load, E_{PV}^{Grid} refers to PV energy exported to the grid, and E_{ST}^{Load} refers to the energy supplied to the load from the ST.

As a result, for each hour t, a pair of values $(SEO_t, Consumption_t)$ is obtained. Once all hourly pairs for the year are available, these pairs are ordered according to the ascending magnitude of SEO_t, and the electricity consumption values are ordered accordingly. In this way, although the original time order is not retained, the temporal correspondence between *SEO* and electricity consumption at each hour is maintained. Under this ordering, *MI* captures the degree of temporal alignment between SEO and electricity consumption across the hours of the year.

The reordered pairs of *SEO* and consumption values are then used to construct two cumulative series, obtained by adding each value to the sum of all previous ones in its respective series. At this stage, the cumulative representation no longer allows identifying the specific time instant at which a given mismatch or temporal misalignment occurred when the Lorenz curve is analyzed on its own. Each cumulative series is subsequently normalized by its own annual total, resulting in values ranging from 0 to 1. Thus, the normalized cumulative SEO is obtained with respect to total annual SEO, and the normalized cumulative consumption with respect to total annual consumption.

These normalized cumulative values, derived from the reordered hourly pairs, define the Lorenz representation used to calculate MI, following [16]. The X-axis corresponds to normalized cumulative electricity consumption, and the Y-axis to normalized cumulative *SEO*. Plotting both cumulative distributions produces the Lorenz curve that represents the temporal relationship between *SEO* and demand. As shown in Figure 4, the Lorenz graph is composed of a 45° line representing perfect temporal alignment and the Lorenz curve showing the actual distribution; the area between them reflects the degree of temporal misalignment between the profiles.

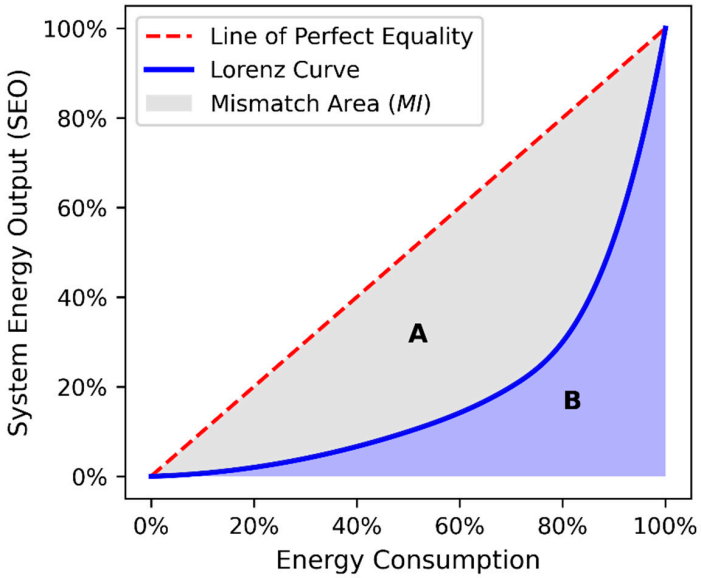


Figure 4. Lorenz curve representation used to compute the Mismatch Index (*MI*) between system energy output (*SEO*) and electricity consumption. The line of equality represents perfect alignment, while the Lorenz curve represents the ordered cumulative distributions. The shaded area (*A*) quantifies mismatch between both curves, whereas area *B* represents the area under the Lorenz curve. The *MI* is calculated by normalizing area *A* by the total area under the equality line (*A* + *B*).

MI is then defined as the area between the diagonal of perfect equality and the resulting Lorenz curve, following the same principle as the Gini coefficient [16]. It can be calculated as the ratio of the mismatch area (*A*) to the total area under the line of equality (*A* + *B*), as expressed in Equation (17)

$$MI = \frac{A}{A + B} \tag{17}$$

MI ranges from 0 (perfect alignment of the ordered cumulative shares) to 1 (maximum misalignment). Lower *MI* indicates that *SEO* and consumption have similar temporal distributions over the analyzed period, reflecting a high degree of energy synchronization. In contrast, high *MI* values indicate lower temporal alignment between generation and consumption, meaning that generation tends to be distributed in periods that do not correspond well to the periods of higher consumption.

MI, therefore, reflects the similarity between the temporal distributions of generation and demand. Since the cumulative Lorenz representation is based on ordered values, the indicator does not allow identifying the specific time instant at which the mismatch occurred when the curve is analyzed on its own and is therefore insensitive to pure time-shift effects. Thus, two profiles may present similar *MI* values even if their peaks occur at different times, provided that their ordered distributions show a similar degree of temporal alignment.

Although the procedure has been described here using the full hourly series obtained from the annual energy balance, the same approach can also be applied after aggregation to other temporal scales, such as monthly averages or hour-of-day averages. In this way, MI can provide complementary views of temporal alignment at different timescales, while making explicit that each level of aggregation highlights some patterns and smooths others. Note that aggregation over months suppresses intra-month and intraday structure, while hour-of-day aggregation suppresses day-to-day and seasonal noise but exposes systematic diurnal misalignment. Used together, these views prevent misleading conclusions from single-scale averaging.

This makes mismatch analysis relevant not only for system performance assessment but also for system design, since it provides information beyond the amount of overlap between generation and demand by showing how both distributions relate over time. In addition, *MI* is a powerful and versatile tool, as it allows the temporal alignment of different variables to be compared with each other. Although this work focuses on comparing the distribution of electricity consumption with that of energy production from the PV system (*SEO*), other alternatives with variables such as solar radiation or electricity tariffs could be employed in mismatch studies.

2.2.2. Positioning of *MI* Among Temporal Matching Indicators

Different temporal matching metrics quantify different aspects of the relationship between PV generation and demand. Overlap metrics, such as *SC* and *SS*, provide intuitive summaries of PV use and grid independence [5], but they primarily quantify annual energy shares and may hide how mismatch is distributed over time [36]. Coincidence-based indicators (e.g., the Load Match Index—LMI, and the Load Cover Factor—LCF) add information on simultaneity within the chosen timestep, while residual-load approaches highlight when deficits and surpluses occur [37]. However, these indicators may not capture how PV generation and demand are relatively distributed over the analyzed period as a whole.

Additionally, in standalone systems, reliability indicators such as loss-of-load probability (LLP) and loss-of-power-supply probability (LPSP) supply analytical methods to determine system reliability—specifically the probability that energy generation cannot meet the load [38,39]; notably, the loss of load probability sizing framework is a well-established research line developed at IES-UPM (the authors' research group), including the foundational contribution by Egido and Lorenzo [40].

In this context, *MI* is introduced as a complementary indicator of *SC* and *SS* to provide distributional information on temporal mismatch that is not explicit in overlap or coincidence metrics. *MI* characterizes how similar the temporal distributions of PV generation and electricity consumption are and therefore acts as an indicator of their structural coincidence, since it is based on normalized cumulative distributions rather than on absolute energy magnitudes, supporting sizing decisions when many configurations exhibit similar *SC* and *SS*.

An illustrative implication is that two PV self-consumption configurations may achieve similar annual *SC* and *SS*, yet differ operationally: one may concentrate surplus PV into a

limited number of high-output hours (surplus-driven behavior), while another distributes smaller surpluses across more hours or exhibits a temporal distribution more consistent with demand. While *SC* and *SS* can be similar, *MI* distinguishes these cases by capturing differences in temporal alignment, thereby improving discrimination within flat regions of sizing maps where many solutions appear equivalent under overlap metrics.

2.3. Economic Assessment Application

The Economic Assessment Application (EAA) evaluates the impact of system size on the overall economic performance of the PV system. Using the hourly energy balance results, EAA quantifies costs and revenues over the system lifetime and maps their effect on four financial indicators: Payback Period (*PBP*), Internal Rate of Return (*IRR*), Levelized Cost of Energy (*LCOE*), and Levelized Profit of Energy (*LPOE*).

As additional input, EAA requires electricity tariffs for importing and exporting energy.

The tool performs a complete parametric mapping across all possible configurations on the parameter interval, considering a set of economic parameters that define the project's financial environment. For each (C_{PV}, C_{ST}) configuration, EAA performs an hourly energy balance over the system's operational lifetime, accounting for the annual PV degradation rate (d_{PV}) and ST degradation rate (d_{ST}). Based on these results, it estimates energy production and quantifies self-consumption (E^{SC}) and exported (E^{export}) energy over the system lifetime, according to Equations (18) and (19), respectively.

$$E^{SC} = \sum_{t=1}^{LT} \left(E_{PV}^{LOAD}(\mathrm{t}) + E_{ST}^{LOAD}(\mathrm{t}) \right) \tag{18}$$

$$E^{export} = \sum_{t=1}^{LT} E_{PV}^{GRID}(\mathrm{t}) \tag{19}$$

From this, the tool computes: (i) total costs, which include capital expenditure (CAPEX) and operational expenditure (OPEX), and (ii) revenues, comprising savings from self-consumption (avoided grid purchases) and the income from energy exports.

2.3.1. Total Costs

For CAPEX, a market survey has been conducted to estimate the unit-cost as a function of system size. Figure 5 shows the PV model unit-cost curves (blue line) with market data (red dots), based on 30 quotations for PV installations obtained from PV installers between 2024 and 2025. PV quotations include PV panels, inverters, mounting structures, and installation labor. In the analyzed quotations, inverter cost represents approximately 17% of total PV CAPEX. A PV unit-cost model has been obtained by nonlinear regression applied to the market quotations.

While PV quotations exhibited a consistent size–cost trend, battery quotations show a substantial dispersion and heterogeneous scope, preventing the identification of a unit-cost regression. Therefore, instead of fitting a size-dependent curve for storage, the analysis adopts a representative battery pack cost of approximately €100/kWh, in line with pack-level cost values reported in the literature, which compile market-based evidence and indicate ongoing cost reductions driven by manufacturing scale and learning effects [41,42].

Therefore, the initial investment (I_0) results from the sum of PV and ST CAPEX costs. The annual OPEX cost (denoted as *C*) covers recurring costs such as preventive and corrective maintenance, monitoring, insurance, and minor replacements. Based on a first-year fixed value (C_1), the OPEX cost increases annually at a rate (g_C) over the system lifetime (*LT*), according to Equation (20).

$$C = C_1 \cdot (1 + g_C)^{LT-1} \tag{20}$$

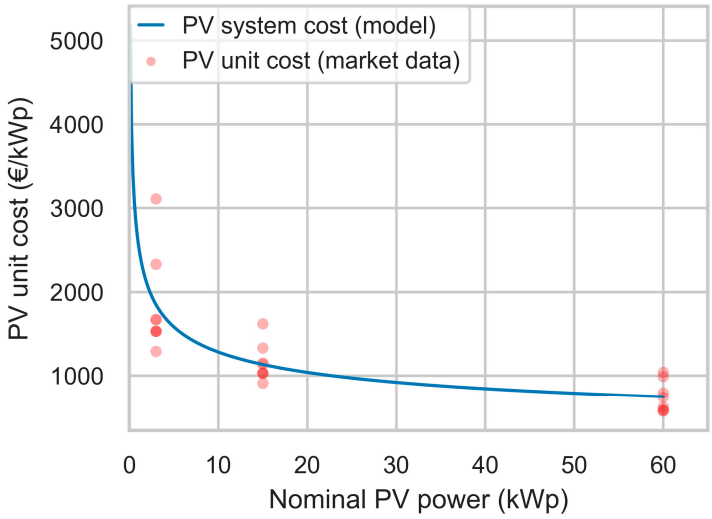


Figure 5. PV unit-cost model used in the Economic Assessment Application (EAA), derived from a market survey (2024–2025). Red markers show 30 collected PV installation quotations, and the blue curve represents the fitted unit-cost model for PV systems (modules, inverter, mounting structures, and installation labor) as a function of nominal PV power (kWp). Note that inverter cost accounts for approximately 17% of total PV CAPEX in the analyzed quotations.

2.3.2. Revenues

The system revenues derive from the hourly simulation of energy flows combined with the applicable electricity tariffs and projected over the system's operational lifetime.

Revenues from self-consumption savings are based on import tariffs (T_{import}), considering annual growth rate (g_T), as expressed by Equation (21).

$$REV_{SC} = \sum_{t=1}^{LT} E^{SC} \times \frac{T_{import}}{(1+g_T)^{(t-1)}} \quad (21)$$

Revenue from exported surplus energy considers the export tariff (T_{export}), as shown in Equation (22).

$$REV_{export} = \sum_{t=1}^{LT} E^{export} \times \frac{T_{export}}{(1+g_T)^{(t-1)}} \quad (22)$$

Together, these cost and revenue components define the energy-economic basis of the system and serve as the foundation for evaluating its financial performance with the calculation of *PBP*, *IRR*, *LCOE* and *LPOE*.

For each economic metric, EAA provides as output a contour map plot according to the viability and competitivity constraints. This output supports target-driven selection and quantitative comparison across configurations.

2.4. System Sizing Application

The System Sizing Application (SSA) aims to size self-consumption PV systems by prioritizing *MI* minimization and then identifying the ST size at which *SC* and *SS* stabilize, subject to economic viability constraints. SSA is implemented as a rule-based, iterative decision procedure over the discretized (C_{PV}, C_{ST}) sizing space, rather than as a continuous mathematical optimization solver. The procedure applies a sequence of priority and threshold decision rules while iteratively adjusting C_{ST} and, if needed, C_{PV}. This approach is not intended to guarantee Pareto-optimality; instead, it prioritizes mismatch reduction (as captured by *MI*) and then identifies technically and economically feasible solutions. Figure 6 summarizes the SSA workflow. As this method also performs economic analysis, it requires as additional inputs the electricity import and export tariffs.

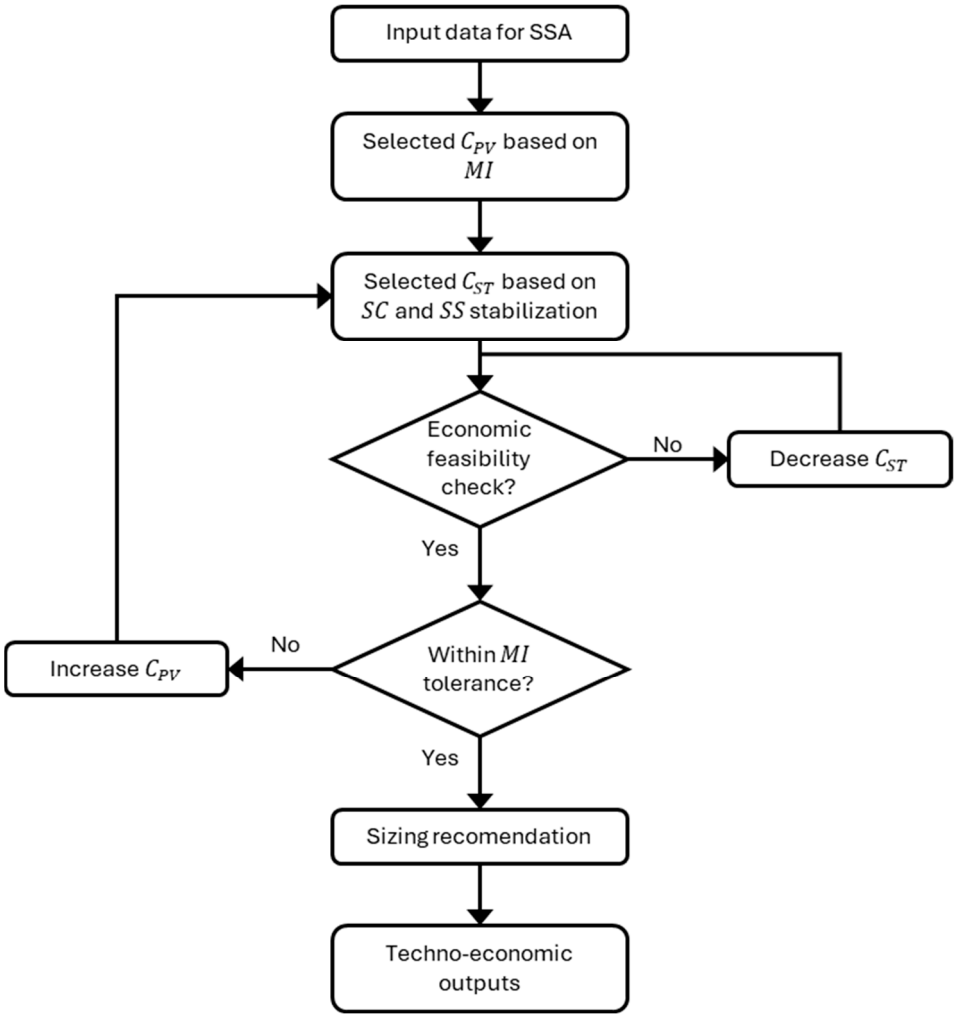


Figure 6. Decision logic of the System Sizing Application (SSA). PV size is selected based on *MI* and ST size based on stabilization of *SC* and *SS* indicators. Economic feasibility is checked by reducing ST size when needed; PV size is increased if *MI* falls outside the predefined tolerance. The output is the final PV–storage configuration and the associated techno-economic indicators.

First, SSA computes *MI* over the entire parameter interval. Since ST size has a direct impact on intraday alignment, SSA focuses on daily *MI*. The method then identifies the minimum stabilization point of *MI* and selects the corresponding C_{PV} value. At this point, a *MI*-tolerance of p (default p = 0.10) is defined to absorb model uncertainty, prevent overfitting to marginal *MI* improvements, and preserve near-equivalent solutions. Within this *MI*-tolerance, C_{ST} remains the free variable for subsequent sizing procedure.

In the second stage, SSA performs an hourly energy-balance simulation while holding C_{PV} fixed at the *MI*-based sizing point. This step determines the C_{ST} value that satisfies the system's stabilization criterion between *SC* and *SS*, completing the technical sizing. The objective is to identify the point from which further increases in ST capacity produce only marginal improvements in *SC* and *SS*. In this way, the stabilization criterion is used as a sufficiency threshold for technical sizing, avoiding oversizing driven by diminishing technical gains. This supports more sustainable sizing by favoring adequate matching between generation and demand instead of unnecessary capacity increases.

In the third stage, SSA applies the economic assessment to evaluate the feasibility of the technically sized configuration. A configuration is considered viable if it meets two conditions:

- $PBP \leq LT$: the system recovers its initial investment within the lifetime period; and

- $IRR \geq r$: the system has a surplus return after accounting for discounting cash inflows.

If the configuration meets these conditions, the method proceeds to the fourth stage; otherwise SSA performs an economic adjustment by decreasing C_{ST} while maintaining the selected C_{PV} until finding the first C_{ST} that meets the two aforementioned conditions. If no configuration achieves feasibility, the method increases C_{PV} in 0.01 increments and repeats the second stage until a feasible solution emerges or confirms that no feasible configuration exists within the parameter interval. This iterative process ensures that the configuration remains as close as possible to the *SC* and *SS* stabilization point while preserving system viability.

Finally, in the fourth stage SSA verifies that the selected configuration remains within the accepted *MI*-tolerance. If the condition is not met, the tool increases C_{PV} by 0.01 and restarts the procedure loop. This iterative process converges toward a balanced configuration that combines mismatch reduction, stabilization of the main technical indicators, and economic viability.

As output, SSA returns a PV–ST configuration report containing all the relevant metrics for this configuration, including technical indicators (*SC*, *SS*, *IE*, *EE*), mismatch indicators (MI_{Daily}, MI_{Annual}), and economic indicators (*PBP*, *IRR*, *LCOE*, *LPOE*).

3. Tool Application to a Residential Case Study

The applications of the tool are illustrated using a case study of a residential consumer from Miedes de Aragón (41.2574° N, 1.4906° W), Spain. Real hourly consumption data from March 2023 to March 2024 has been obtained from [33] as energy demand input.

As meteorological input, irradiance and ambient temperature series from a Typical Meteorological Year (TMY) by PVGIS [32], to reduce sensitivity to interannual variability in solar resource assessment, have been obtained using the location of Miedes de Aragón as the reference point. Effective irradiance has been estimated through SISIFO tool [43] considering PV modules tilted 30° and oriented south (azimuth 0°). A constant system efficiency of 90% has been considered to account for balance-of-system losses: 92% for module-side losses (mismatch, soiling, incidence-angle, spectral, and cabling losses) combined with 98% inverter efficiency.

Figure 7 presents the average hourly temperature, effective irradiance, and energy consumption for this case study. In the specified period, the annual energy consumption has been 6837 kWh, with a daily mean of 18.73 kWh, average temperature of 11.7 °C, and effective annual irradiance of 1788 kWh/m^2. Under these conditions, a $C_{PV} = 1$ results in a PV generator of 4.0 kWp, and a $C_{ST} = 1$ corresponds to a ST of 18.73 kWh.

As tariffs input, the hourly PVPC tariff [44] (Voluntary Price for the Small Consumer, Spain's regulated time-varying tariff for small consumers) for the same energy consumption period has been obtained from [45] to mirror real operating conditions and preserve intraday variability and seasonality. Figure 8 presents the daily tariff profile as hourly averages with 95% error bands. In the period, the average import tariff (blue line) was €138/MWh, while the export tariff (orange line) averages €77/MWh.

3.1. Energy Flow Application Results

Figure 9 presents the energy flow results of the case study. The plot visualizes performance indicators on the y-axis, while x-axis sweeps either with C_{PV} (with C_{ST} fixed) or C_{ST} (with C_{PV} fixed). Each parameter varies individually, allowing users to understand the implications of system size adjustments.

Figure 9a presents a no-ST case, allowing the user to observe how performance indicators respond to C_{PV} variations: *SC* (green dosh-dot line) decreases while *SS* (blue dotted line) rises with C_{PV} increasing, overlapping when $C_{PV} = 1$; their slopes tend to

smooth out as C_{PV} increases, causing EE to undergo near-exponential growth in the absence of ST. This pattern shows that further capacity increases have limited impact on reducing grid dependency.

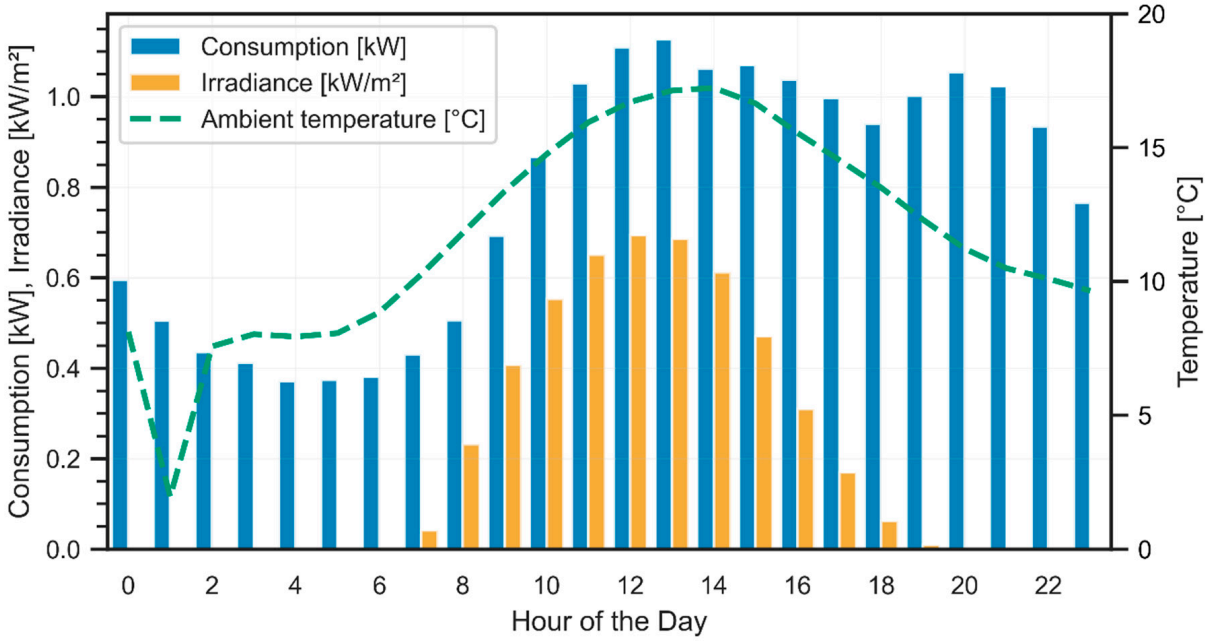


Figure 7. Hourly averages of consumption, effective irradiance and ambient temperature for the case study. Consumption data has been obtained from Datadis [33], a unified Spanish platform that provides end users access to smart-meter electricity consumption records (March 2023–March 2024). Meteorological data (irradiance and ambient temperature) correspond to a PVGIS [32] Typical Meteorological Year (TMY) series defined for the reference location of Miedes de Aragón. Effective irradiance corresponds to the PV plane (tilt 30°, south-facing) used in the PV production model.

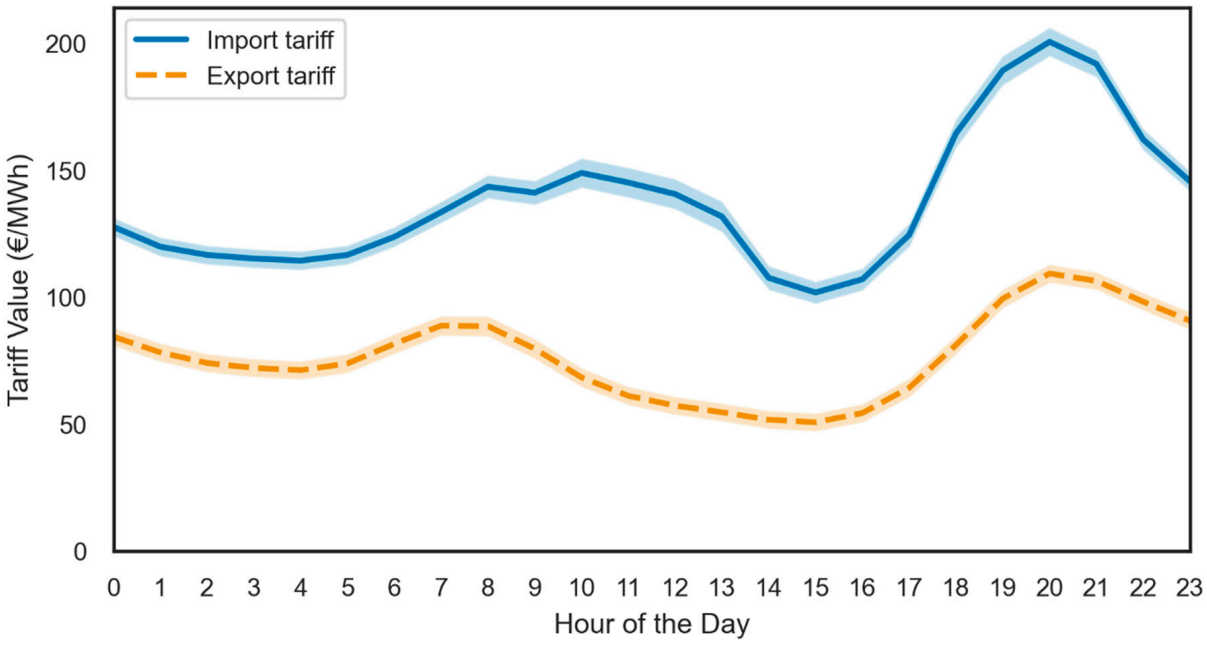


Figure 8. Average daily profile of PVPC import and export costs (March 2023–March 2024), obtained from [45]. Solid lines show hourly averages and shaded bands represent the 95% interval, illustrating intraday variability relevant for the techno-economic assessment.

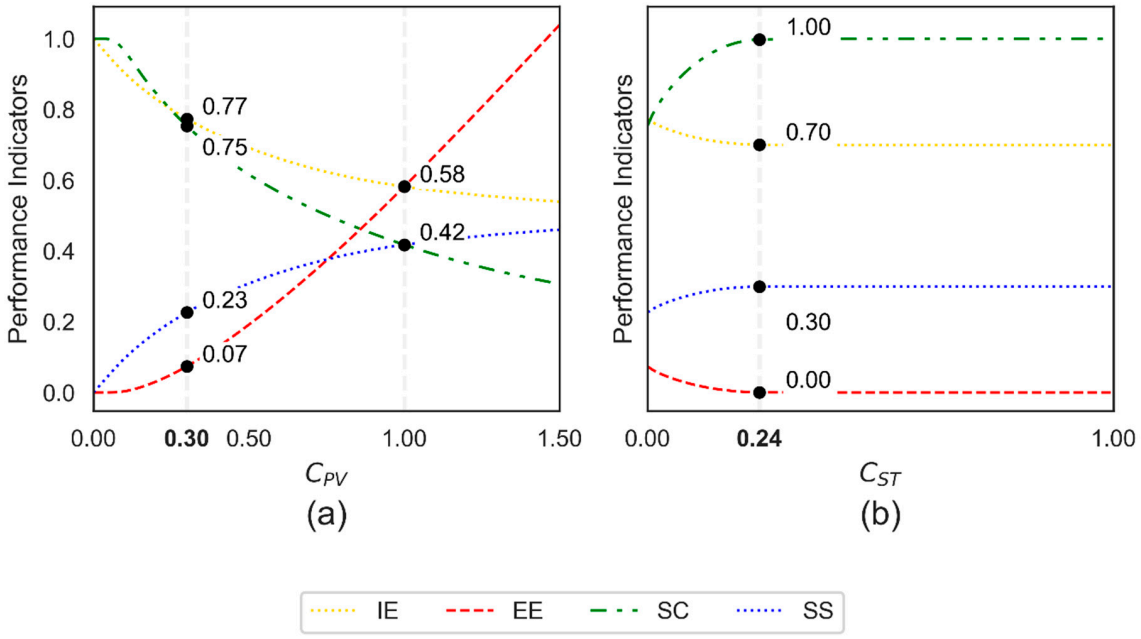


Figure 9. Energy flow analysis of the *SC*, *SS*, *IE* and *EE* performance metrics for the residential case study: (**a**) No-ST case (C_{ST} = 0) varying C_{PV}, and (**b**) a fixed PV size (with C_{PV} = 0.30) varying C_{ST}, highlighting the stabilization point used to avoid oversizing under the EFA criterion.

In addition, the energy flow graph proves particularly useful for target-driven analysis of specific metrics. As an example, while the $C_{PV} = 1$ results in a *SS* and *SC* of 0.42, a hypothetical user-selected target of *SC* = 0.75 could be met with a 70% reduction in PV size ($C_{PV} = 0.30$), obtaining *SS* to 0.23 (Figure 9a). This means that a balanced approach can be taken to choose a C_{PV} that meets the desired performance requirements without oversizing, ensuring the system remains operationally efficient.

Similarly, users can explore how parameters behave when adding ST by fixing a C_{PV} as in Figure 9b. In general, larger C_{ST} represents greater grid independence; however, extra ST results in negligible benefits, which highlights the importance of identifying the C_{ST} at which the system reaches equilibrium. In a hypothetical case where the user preselects $C_{PV} = 0.30$, the system reaches such equilibrium at $C_{ST} = 0.24$, as shown in Figure 9b. Compared to the no-ST case at the same C_{PV}, adding ST may increase *SC* by 33.3% (from 0.75 to 1.00) and *SS* by 30.4% (from 0.23 to 0.30).

Considering the monthly variability of both PV generation and electricity demand, system performance is assessed at monthly and seasonal scales in Figure 10. Monthly results (Figure 10a) show that *SC* remains close to unity throughout the year (0.98–1.00), indicating that PV electricity is almost entirely absorbed locally under the analyzed configuration, with only a minor deviation in August ($SC = 0.98$). In contrast, *SS* shows a substantially higher temporal variability (0.16–0.57 on a monthly basis), reflecting changes in the balance between PV availability and electricity demand across the year. The lowest *SS* values are observed in winter months (December–February), while the highest *SS* occurs in early autumn (September), when the generation–demand match is comparatively more favourable. Seasonal aggregation, shown in Figure 10b, confirms this pattern: SS reaches its minimum in winter (0.19) and its maximum in autumn (0.42), with intermediate values in spring and summer (0.33 and 0.31).

The 3D surface output (Figure 11) maps *SC* fluctuations and highlights the combinations that maximize it. The iso-curve output (Figure 12) shows equivalent combinations (C_{PV}, C_{ST}) in terms of *SC*; for example, other combinations that achieve *SC* of 75% besides (0.30, 0.0) are the (0.54, 0.11) and (0.74, 0.24).

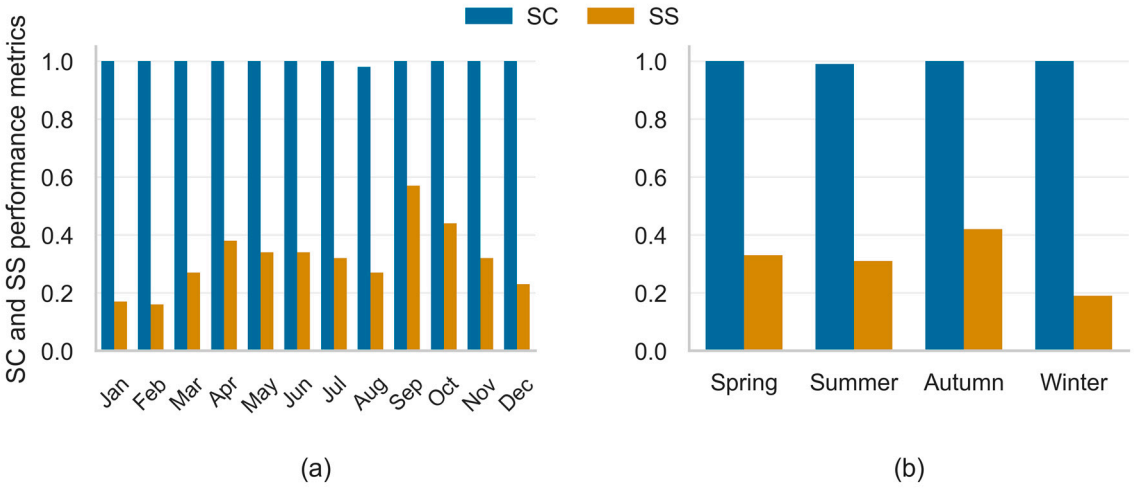


Figure 10. Monthly and seasonal self-consumption performance. (**a**) Monthly *SC* and *SS*. (**b**) Seasonal aggregation of *SC* and *SS* (Spring, Summer, Autumn, Winter).

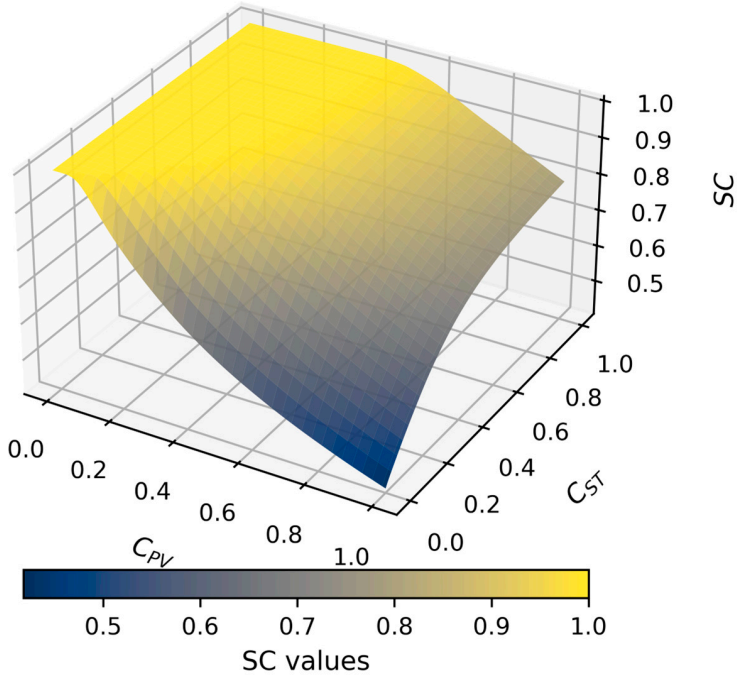


Figure 11. Surface map of self-consumption (*SC*) over the normalized sizing space (C_{PV}, C_{ST}) for the case study, obtained from hourly energy-balance simulations. The surface highlights regions where SC saturates, supporting identification of diminishing returns with increasing PV and ST size.

3.2. Consumption–Generation Alignment Application Results

CGA has been applied for the case study considering the previously selected no-ST user-selected system ($C_{PV} = 0.30, C_{ST} = 0$). Figure 13 presents the Lorenz curve result. The annual analysis (Figure 13a) shows a small mismatch area, obtaining a $MI_{Annual} = 0.15$, suggesting a well-balanced alignment over the year. In contrast, Figure 13b presents the daily assessment and returns a larger mismatch area ($MI_{Daily} = 0.63$), indicating weak coincidence between the distributions during nearly half of the hours of the year.

To complement the Lorenz view, Figure 14 shows the normalized mean-profile plot, comparing energy consumption (blue bars) and *SEO* (yellow bars). The annual view (Figure 14a) indicates few shortfalls and surpluses periods (October–December and July–August, respectively), even under overall good annual alignment. However, the daily view

(Figure 14b) shows pronounced gaps during most of the day, suggesting potential benefits from ST solutions or demand-shifting strategies.

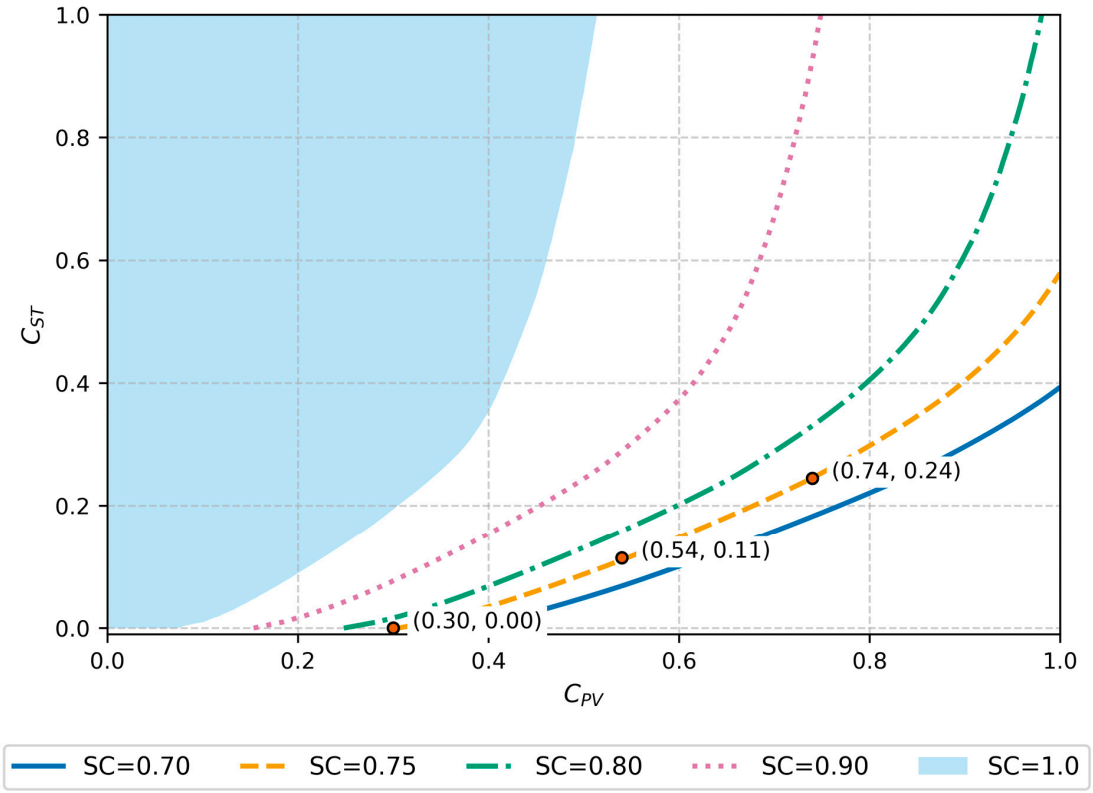


Figure 12. Isometric curves of *SC* as a function of C_{PV} and C_{ST} for the case study, showing alternative PV–ST combinations that achieve the same *SC* value. Marked examples illustrate how storage can trade off with PV size to meet target-driven *SC* levels.

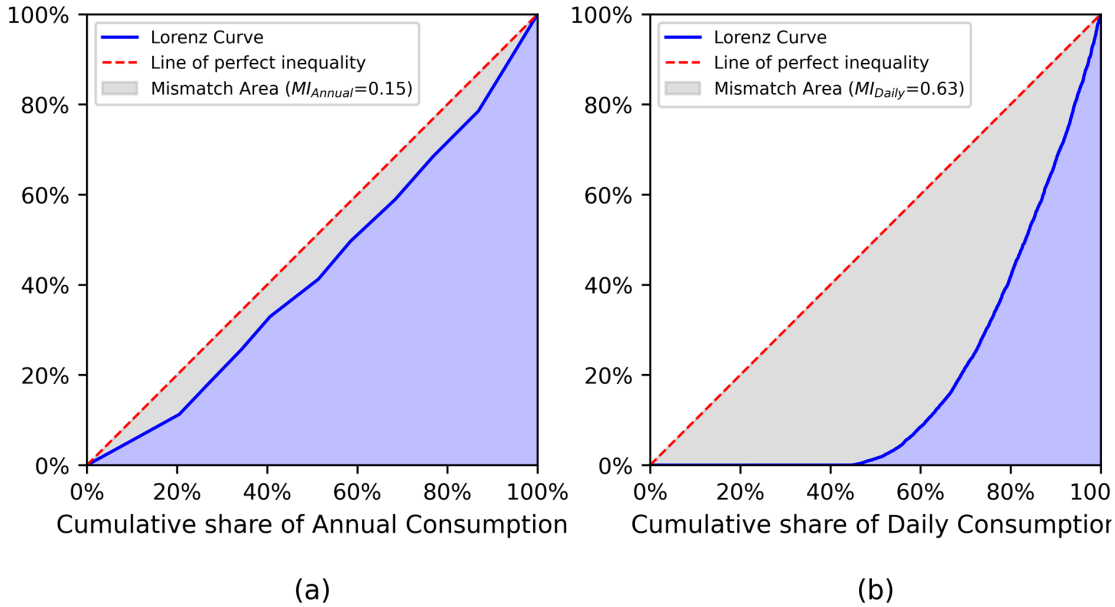


Figure 13. MI assessment for the baseline configuration without storage (C_{PV} = 0.30, C_{ST} = 0). (**a**) Annual view using monthly mean profiles; (**b**) daily view using hour-of-day mean profiles. Shaded mismatch areas illustrate how aggregation scale affects the observed alignment. The gray shaded area represents the mismatch (*MI*), whereas the blue area represents the area under the Lorenz curve.

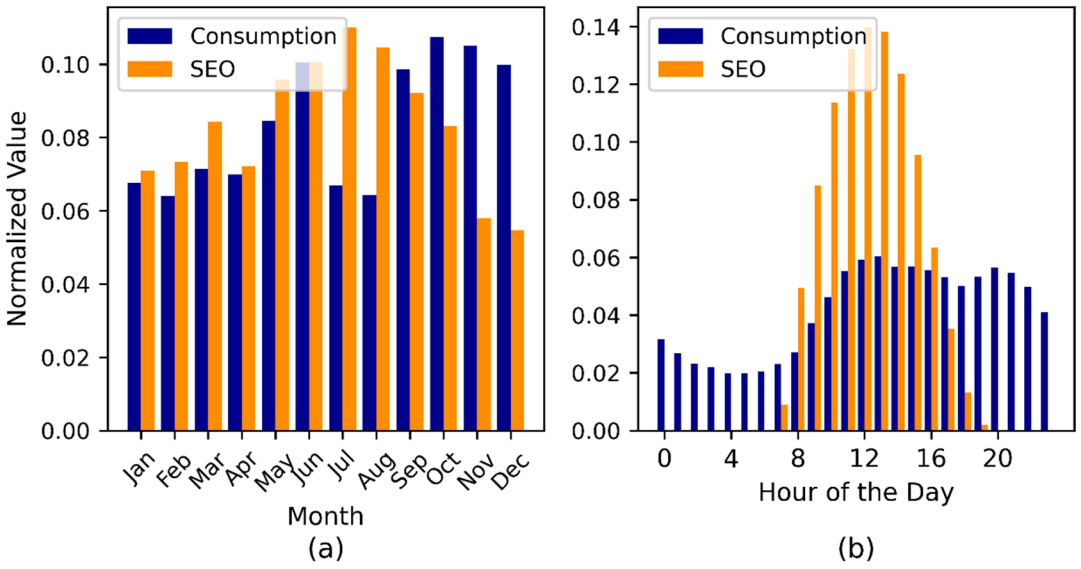


Figure 14. Normalized mean profiles of electricity consumption and system energy output (*SEO*) for the case study considering the baseline system without ST (C_{PV} = 0.30, C_{ST} = 0). (**a**) Monthly mean (annual view) highlighting seasonal surplus/shortfall periods; (**b**) mean by hour of day (daily view) highlighting systematic intraday mismatch relevant for storage and demand-shifting strategies.

When adding ST (C_{PV} = 0.30, C_{ST} = 0.24), Figure 15 shows the impact of ST on daily *MI* analysis, improving MI_{Daily} by 20.6%, as shown in Figure 15a; meanwhile, the normalized annual mean hourly profile in Figure 15b also reflects the battery contribution, prolonging system supply into night hours. Note that even though the battery follows a maximum-discharge logic (it discharges as much as possible each hour when PV is absent or insufficient), its discharge does not perfectly track the load in Figure 15b because this curve represents an annual mean hourly profile, which introduces a phase lag.

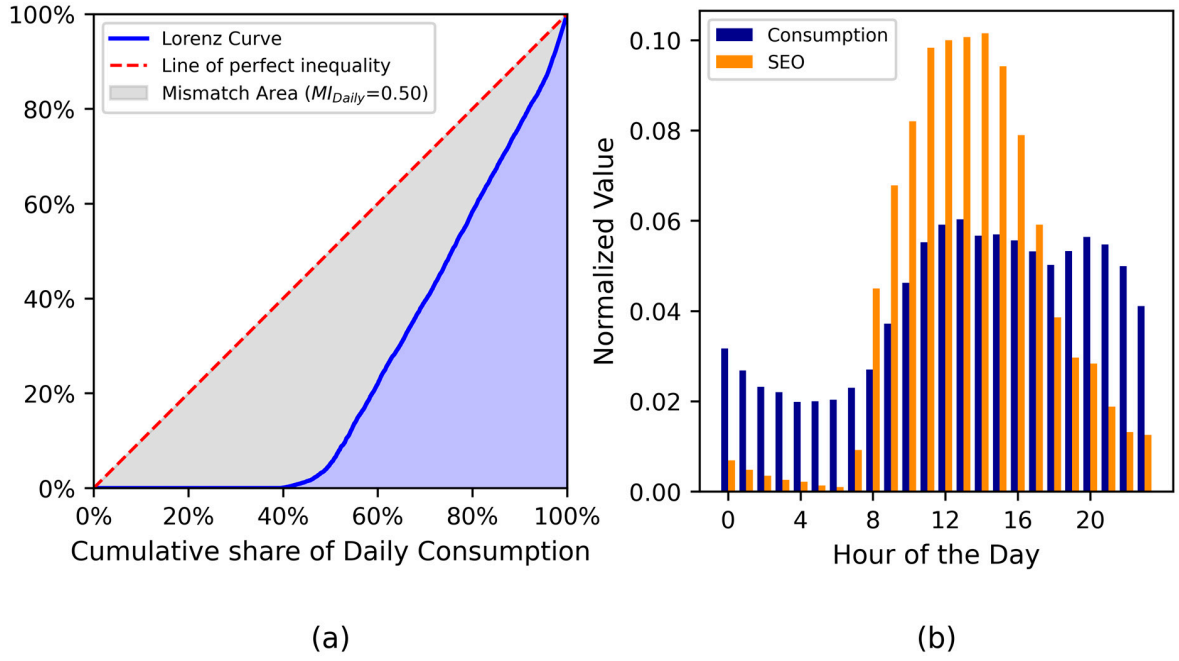


Figure 15. Impact of storage on coincidence alignment for C_{PV} = 0.30 when adding storage (C_{ST} = 0.24). (**a**) Lorenz curve (daily view) showing the reduction in the gray mismatch area and *MI*, while the blue area represents the area under the Lorenz curve; (**b**) normalized hour-of-day mean profiles of consumption and *SEO* illustrating the extension of supply into evening hours.

3.3. Economic Assessment Application Results

The Economic Assessment Application (EAA) has been performed considering the economic parameters summarized in Table 1, adopting an economic evaluation baseline for Spain. The project lifetime is set to 20 years, consistent with common planning horizons adopted for residential PV investment appraisal and with the warranty-driven lifetime assumptions used in the literature [46]. The discount rate of 3% reflects a baseline cost of capital for the study context [47], and tariff growth of 2.17% follows the compound annual growth rate over 2015–2024 [48]. PV degradation is set to 1% per year as a conservative value within commonly reported ranges for crystalline-silicon PV [49]. Operating expenditures are represented by a first-year OPEX $C_1 = 0.65\%$ of CAPEX [50], consistent with literature values for PV system operation and maintenance, and an annual OPEX growth of 3% to reflect the escalation of service and maintenance costs over the project lifetime [51].

Table 1. Summary of economic parameters used in the simulations.

Parameter	Value	Reference
PV-ST system lifetime (LT)	20 years	[46]
Discount rate (r)	3% per year	[47]
Tariff annual growth (g_T)	2.17% per year [1]	[48]
PV degradation (d_{PV})	1% per year	[49]
First-year OPEX (C_1)	0.65% of CAPEX	[50]
$OPEX$ annual growth (g_C)	3% per year	[51]
Inverter and ST replacement	At year 10	[52,53]
ST degradation (d_{ST})	2% per year	[53,54]
Country Regulation	Spain	[55]

[1] Calculated as a compound annual growth rate (CAGR) based on the last ten years (2015–2024) and does not reflect the high year-to-year volatility of market prices.

Battery aging and inverter replacement add uncertainty to long-term PV–ST economics. In related techno-economic studies, inverter and ST lifetime is often set to 10 years, implying at least one replacement could occur within 20 years [52,53]. Battery ageing is represented through an average degradation rate of 2.0% per year for Li-ion, consistent with techno-economic modelling assumptions reported in the literature [53,54].

Following the Spanish self-consumption regulation [55], a monthly compensation cap for surplus generation has been applied: remuneration for exported energy may not exceed the cost of imported grid energy. Therefore, once both values match, any additional surplus flows to the grid without further compensation. Note that no loans or subsidies have been considered.

Based on these parameters, the EAA has been applied to the case study evaluating all PV-ST possible configurations. Figure 16 reports the output contour maps for the four indicators considered (PBP, IRR, $LCOE$, and $LPOE$), providing a complementary perspective. Figure 16a shows the PBP ranging from 11–20 years. Blank PBP regions mark configurations that fail to recover within the project lifetime. Figure 16b shows the IRR behavior, ranging up to 6.5%, while blank IRR area indicates non-profitable configurations ($IRR < r$, with $r = 3\%$). Figure 16c shows a $LCOE$ with values below €140/MWh; blank area represents higher values that are not competitive (average import tariff for the period was €138/MWh). Finally, Figure 16d shows $LPOE$, ranging up to €21/MWh.

Results indicate that not all PV–ST configurations achieve economic viability in this case study. In general, configurations up to $C_{PV} \cong 0.6$ progressively lose cost-effectiveness as storage capacity increases: the PBP exceeds the 20-year system lifetime and the $LCOE$ rises above 140 €/MWh. In addition, configurations with an IRR below the discount rate also result in a negative $LPOE$. On the other hand, the results also highlight regions where PV-ST configurations maximize IRR and $LPOE$ and minimize PBP and $LCOE$ (highlighted

in Figure 16 as the light-colored, yellowish areas of the contour maps), indicating, respectively, higher relative return, greater lifetime profit per unit of energy, faster recovery of the initial investment and lower unit electricity costs.

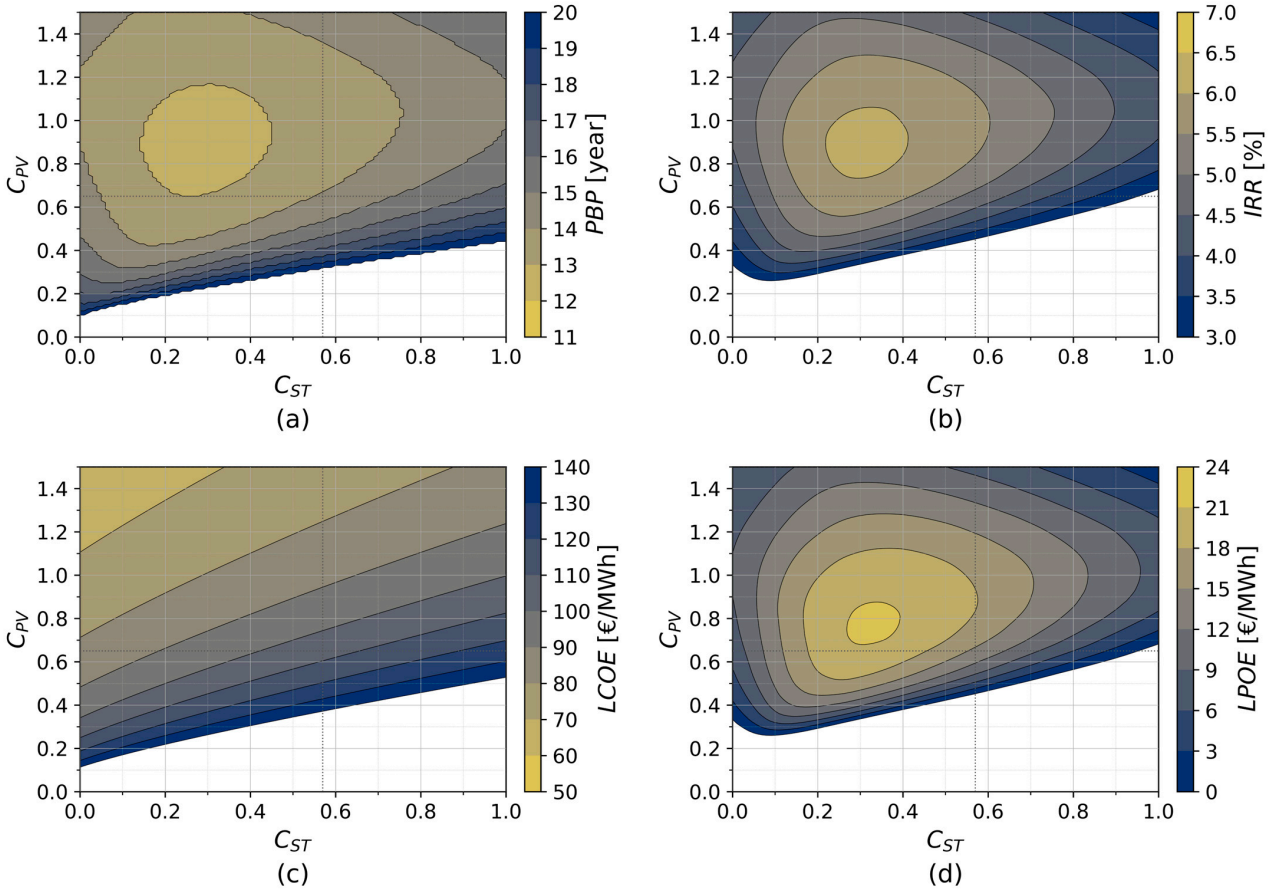


Figure 16. EAA contour maps over (C_{PV}, C_{ST}) for the residential case: (**a**) payback period (*PBP*), (**b**) internal rate of return (*IRR*), (**c**) levelized cost of energy (*LCOE*), and (**d**) levelized profit of energy (*LPOE*). Color shading is oriented so that lighter tones indicate more favorable outcomes (lower *PBP* and *LCOE*; higher *IRR* and *LPOE*). Blank regions indicate configurations that do not meet the corresponding viability or competitiveness criteria.

Together, the EAA outputs allow even non-expert users to visually understand how different system sizes affect cost-effectiveness, profitability, and electricity costs, helping to identify more advantageous configurations according to their financial priorities. For instance, Table 2 compares the user-selected system with and without ST. In this case, adding ST still results in a *PBP* within the system lifetime and preserves a competitive *LCOE*, but the system still remains non-viable, with *IRR* lower than the discount rate ($r = 3\%$) and a negative *LPOE*. This type of comparison helps users clearly identify when ST supports their financial goals and when it mainly adds cost without sufficient economic return.

Table 2. Comparison of EAA results considering user-selected system with and without ST.

	No-ST System (C_{PV} = 0.30,C_{ST} = 0)	**PV-ST System** (C_{PV} = 0.30,C_{ST} = 0.24)
PBP [years]	16	16
IRR [%]	2.80	2.81
LCOE [€/MWh]	109.92	125.94
LPOE [€/MWh] [1]	−1.59	−1.70

[1] Note that a negative LPOE, when considering the battery system (ST), indicates a negative net benefit per unit of electricity generated.

3.4. System Sizing Application Results

The System Sizing Application (SSA) has been applied to the case study with the aim of obtaining a PV–ST configuration that minimizes mismatch (MI), identifies the stabilization point of SC and SS, and remains economically viable. Figure 17 displays representative iso-curves of MI_{Daily} as a function of (C_{PV}, C_{ST}) pairs, illustrating how different size combinations affect mismatch in the hourly view. The minimum MI-stabilization point occurs at the $C_{ST} = 1$ curve when $C_{PV} = 0.75$, where $MI_{Daily} = 0.30$. Based on this point, the MI-tolerance (previously set at 10%) has been set to a maximum value of 0.40.

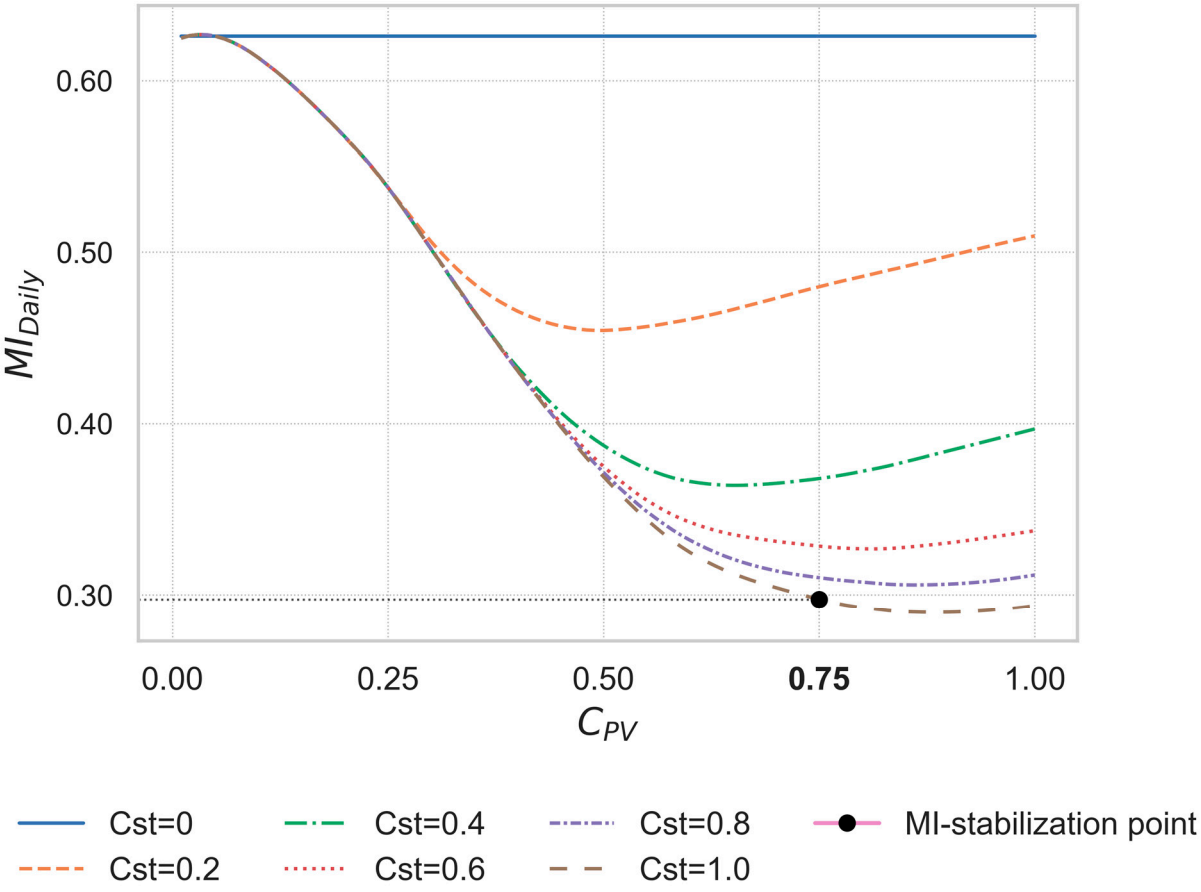


Figure 17. MI_{daily} iso-curves across the (C_{PV}, C_{ST}) sizing space for the residential case, computed from the full annual hourly time series (8760 h). The highlighted point indicates the MI stabilization region used by SSA to define the PV size.

Fixing $C_{PV} = 0.75$, SSA identifies the C_{ST} at which the energy flow stabilizes; that is, the point from which further increases in ST capacity lead only to marginal improvements in SC and SS, as shown in Figure 18. This point occurs at $C_{ST} = 0.65$, delivering high local utilization ($SC = 0.87$) and substantial autonomy ($SS = 0.66$). These results define the technical sizing outcome.

In the economic analysis the technically sized configuration meets both viability criterion. IRR results above the discount rate (4.93% $\geq$ 3%) while also satisfying the PBP condition (14 years $\leq$ 20 years). Therefore, no configuration adjustment is needed, thereby concluding SSA.

Table 3 summarizes the performance and economic outputs of the final configuration. The mismatch target is met, with the daily coincidence reaching the minimum stabilization point $MI_{\text{Daily}} = 0.30$, and the annual coincidence remaining consistent ($MI_{Annual} = 0.15$). As no economic adjustment was needed, the stabilization-based technical sizing was

preserved, ensuring consistency with the technical objective of increasing local use of PV generation and independence of the grid. Economically, besides the configuration meeting viability criteria, the *LCOE* achieves a competitive value 25.68% lower than the average electricity import tariff in the considered period (€138/MWh), and, although the *LPOE* has a low result, it has a positive value which indicates profitability. Overall, the SSA delivers a configuration that fulfills its intended objectives, balancing temporal alignment, technical performance and economic viability for the case study. In addition, the selected configuration is consistent with a more sustainable sizing rationale, as it improves the effective use of locally generated PV electricity while avoiding unnecessary capacity increases that could lead to surplus generation without proportional technical benefit. This outcome illustrates the tool's capacity to translate hourly energy-balance simulations into actionable sizing recommendations under realistic tariff and cost assumptions.

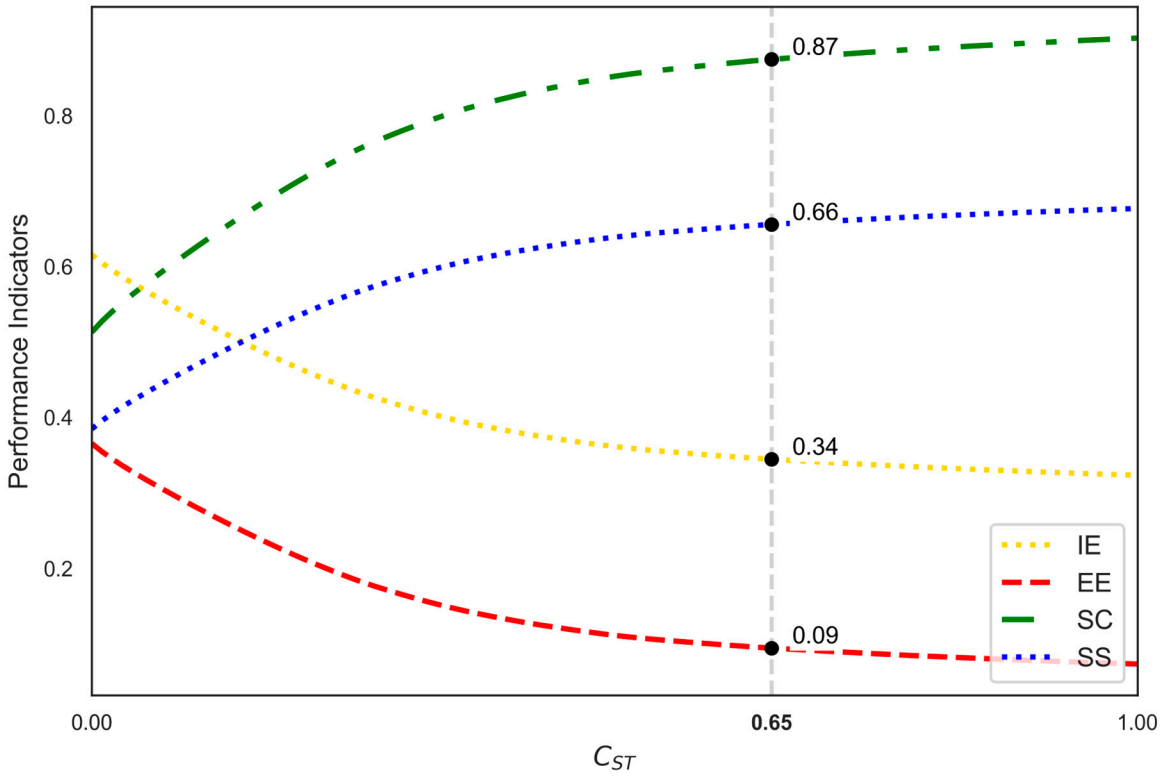


Figure 18. Energy balance applied by SSA for the selected PV size (C_{PV} = 0.75), varying C_{ST} to identify the *SC* and *SS* stabilization point. The highlighted point corresponds to the ST size adopted after applying the technical stabilization criterion).

Table 3. Summary of SSA output for the case study.

Performance Indicators	SSA Selected System	Economic Indicators	SSA Selected System
PV Generator [kWp]	3.24	CAPEX [k€]	7.07
ST capacity [kWh]	12.18	OPEX [k€]	3.49
MI_{Daily}	0.30	Revenue [k€]	15.00
MI_{Annual}	0.15	*NPV* [k€]	1.36
SC	0.87	*PBP* [years]	14
SS	0.66	*IRR* [%]	4.92
IE	0.34	*LCOE* [€/MWh]	102.78
EE	0.09	*LPOE* [€/MWh]	14.56

4. SSA Application to an Energy Community Case Study

The tool offers additional capabilities when used for designing PV systems integrated into renewable energy communities (RECs), considering dynamic energy sharing, where PV electricity is allocated at each timestep based on participants' demand [12]. For instance, when RECs operate in rural areas, it is often more efficient to group self-consumption systems into a single collective PV system than to install several individual systems for each prosumer. While grouping is often associated with reduced investment and operating costs, the performance of an aggregated PV system compared with several individual PV systems must be studied.

The authors have had access to energy consumption data from REC [31], established in Calatayud County, northern Spain. Ten prosumers from one of the villages in which the REC operates in the Calatayud County, Miedes de Aragón, have been selected.

A comparative assessment between two implementation scenarios for the Miedes de Aragon case is presented: (i) individual systems, where each participant installs an independent PV generator and ST, and (ii) a collective configuration with a centralized PV-ST system. The SSA has been applied to both configurations.

4.1. Miedes de Aragon Case Study

An energy consumption analysis of the ten consumers from the Miedes de Aragón case is presented in Table 4 at individual and aggregated levels, based on the annual consumption between March 2023 to March 2024 obtained from [33]. Annual aggregated consumption totals 30,827 kWh, while average consumption per consumer reaches 3083 kWh (84.46 kWh/day and 3.51 kWh/h). Individual consumption shows high variability ranging 237–6837 kWh and resulting in a coefficient of variation (CV) of 60.6%. The largest consumer (C8) represents 22.2% of the total demand, while the smallest (C6) accounts for only 0.8%. The aggregated daily profile in Figure 19 shows the average hourly consumption as a stacked bar chart: each bar gives the total average hourly demand, and the colored segments indicate each consumer's relative contribution. For reference, the consumer from the previous study case corresponds to C8.

In the community scenario, energy sharing takes place at village level along the low-voltage feeder, without crossing the MV/LV transformer, in line with the Spanish self-consumption framework [55]; therefore, internal distribution losses are not considered. Additionally, since this scenario represents an energy-community, O&M costs include a community management fee of *c*€2.20/kWh of PV energy produced, based on the actual management cost of the energy community analyzed in this study.

Table 4. Main energy consumption metrics by individual consumer and aggregated consumption for Miedes de Aragón case study, based on 2024 data.

Consumer	Annual Consumption [kWh]	Daily Mean [kWh/Day]	Hourly Mean [kWh]	Share of Total Consumption [%]
C1	3559	9.75	0.41	11.5
C2	4752	13.02	0.54	15.4
C3	4882	13.38	0.56	15.8
C4	2706	7.41	0.31	8.8
C5	3462	9.48	0.4	11.2
C6	237	0.65	0.03	0.8
C7	1430	3.92	0.16	4.6
C8	6837	18.73	0.78	22.2
C9	403	1.10	0.05	1.3
C10	2560	7.01	0.29	8.3
Aggregated	30,827	84.46	3.51	100.0

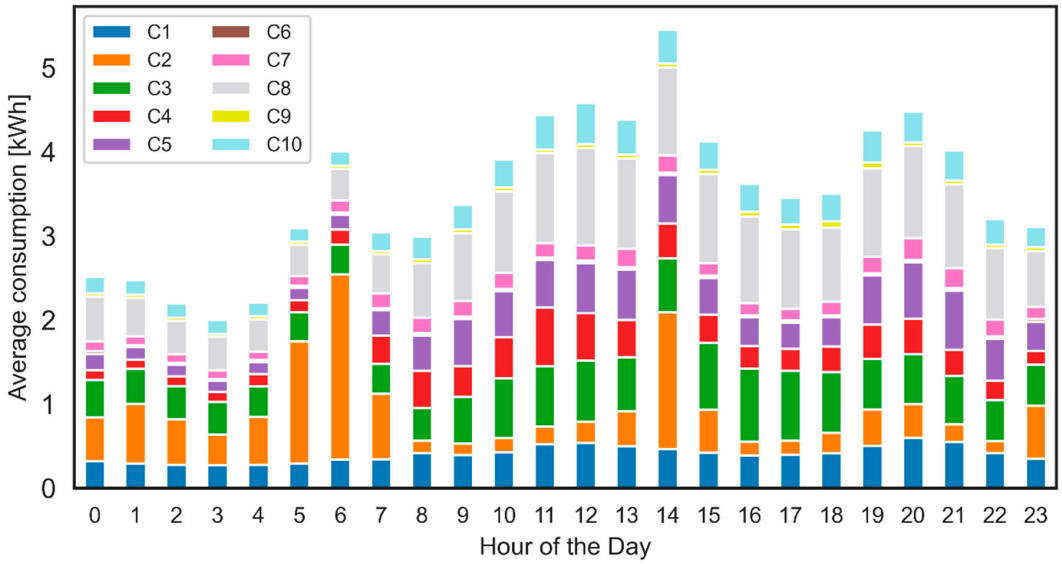


Figure 19. Aggregated average hourly consumption profile of the ten prosumers (stacked bars), showing each participant's contribution to the community demand by hour of day. The plot highlights demand concentration periods that influence PV–ST sizing under individual versus centralized configurations. Data obtained from [33].

4.2. SSA Results

To compare system sizes and economic viability between scenarios, SSA has been applied based on environmental data from Miedes de Aragón nearest meteorological station and the tariffs input from the same consumption period (described in Section 3). Table 5 consolidates SSA outputs for both the individual and collective configurations.

Table 5. SSA outputs for the Miedes de Aragón case study: individual systems and centralized system with aggregated demand.

	C1	C2	C3	C4	C5	C6	C7	C8	C9	C10	Individual System Total [1]	Centralized System
System Viability	Yes	No	Yes	Yes	Yes	No	No	Yes	No	Yes	NA	Yes
PV [kWp]	2.09	1.68	2.66	1.54	1.82	0.13	0.69	3.24	0.22	1.42	15.50	15.79
ST [kWh]	7.41	7.81	8.56	4.75	5.97	0.44	2.94	12.18	0.78	4.07	54.90	47.30
MI_{Daily}	0.21	0.50	0.24	0.19	0.27	0.23	0.26	0.30	0.25	0.24	0.50	0.31
MI_{Annual}	0.07	0.40	0.13	0.13	0.19	0.07	0.10	0.15	0.05	0.09	0.40	0.17
SC	0.90	0.80	0.91	0.90	0.89	0.90	0.88	0.87	0.88	0.89	0.80	0.91
SS	0.84	0.45	0.79	0.81	0.74	0.77	0.67	0.66	0.77	0.78	0.45	0.74
IE	0.16	0.55	0.21	0.19	0.26	0.23	0.33	0.34	0.23	0.22	0.55	0.26
EE	0.09	0.11	0.08	0.09	0.09	0.08	0.09	0.09	0.10	0.10	0.11	0.07
CAPEX [k€]	5.05	4.49	5.95	3.96	4.51	0.66	2.28	7.07	0.99	3.70	38.64	22.37
OPEX [k€]	2.39	2.22	2.80	1.78	2.08	0.27	1.04	3.49	0.41	1.64	18.11	17.86
Revenue [k€]	7.44	6.71	8.74	5.74	6.58	0.92	3.32	10.56	1.40	5.34	56.75	40.23
PBP [years]	15	20	14	15	15	32	20	14	27	16	32	8
NPV [k€]	0.66	−1.09	1.26	0.17	0.45	−0.41	−0.62	1.37	−0.50	0.09	1.37	20.06
IRR [%]	4.31	0.31	5.09	3.43	4.02	−5.16	−0.03	4.92	−3.32	3.25	−5.16	10.84
LCOE [€/MWh]	112.53	125.50	104.13	118.32	114.84	231.32	153.23	102.78	199.00	119.18	102.78	77.98
LPOE [€/MWh]	10.92	−22.45	16.35	3.75	8.62	−110.44	−30.95	14.56	−77.78	2.22	−110.44	43.92

[1] Individual System Total refers to the sum of individual systems and costs, considering maximum MI_{Daily} and MI_{Annual}, minimum *SC*, *SS*, longest *PBP*, and lowest *IRR*, *LCOE*, and *LPO*.

However, in the individual scenarios, four consumers result in non-viable systems, reaching a maximum *PBP* of 32 years and a minimum *IRR* of −5.16%; on the other

hand, the collective scenario resulted viable, with a PBP of 8 years and a IRR of 10.84%. Subsequent sections provide detailed analysis of these outcomes.

4.3. Performance Assessment

Figure 20 compares indicators across consumers using boxplots, with a green diamond marking the centralized case. At individual level, SC clusters around 0.89 with low dispersion (Relative Standard Deviation—RSD of 3.3%), signaling consistent local use of PV across consumers and, consequently, limited surplus. Accordingly, EE remains low, with a mean of 0.09; SS spans 0.44–0.84 and centers near 0.73, indicating lower reliance on the grid.

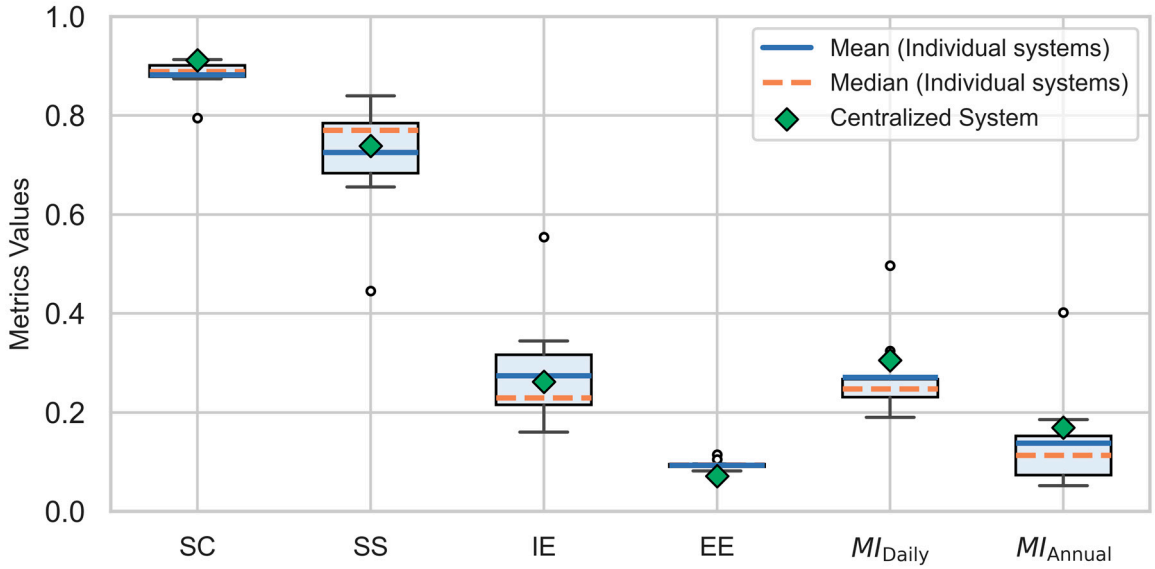


Figure 20. Distribution of technical and mismatch indicators across individual prosumers (boxplots) compared with the centralized configuration (green marker): SC, SS, IE, EE, MI_{daily} and MI_{annual}. Boxplots summarize inter-consumer variability; the marker shows the indicator values obtained for the aggregated-demand (centralized) sizing. Circles indicate outlier values.

When aggregating consumption, the centralized configuration shifts the indicators slightly in its favor: SC increases by 14.6%; SS reaches 0.74, increasing 39.7%; grid dependence declines, with IE decreasing by 112.0% and EE by 65.8%. However, for most consumers, mismatch weakens under aggregation. On the annual analysis, MI_{Annual} rises from 0.14 (individual mean) to 0.17 (centralized), maintaining a good monthly alignment. On the daily analysis, MI_{Daily} increased 13.7% in comparison to the individual mean (0.27), achieving 0.31.

4.4. Economic Assessment

On the economic analysis, load aggregation reduced CAPEX by 42.1% and OPEX by 1.4% compared to the sum of individual systems. The OPEX reduction remains limited, as the community management fee scales with the shared system's energy output. Furthermore, due to the SSA approach based on the stabilization of SC, revenues rely mainly on self-consumption savings in both scenarios (about 95%); however, the centralized system generates 29.1% more revenues. In general, the centralized system significantly increases profits over a 20-year period: the NPV rises from €1.37k for individual systems to €20.06k for the centralized system, an increase of almost 15 times.

The investment performance analysis includes viability constraints based on a project LT of 20 years and r = 3%. Figure 21 plots IRR against PBP (quadrants delimited by $IRR \geq r$ and $PBP \leq LT$). At the individual level (circle markers), the two systems did not

achieve any of the viability constraints, resulting in negative IRR and PBP higher than 20 years. Two additional systems reach PBP values close to the lifetime limit, while IRR remains close to zero. The remaining individual systems achieve similar performance: PBP around 15 years and a positive IRR up to 5%. In the comparison scenario, the centralized system (diamond marker) is highlighted with an IRR of 10.8%, 3.6 times higher than r, and a PBP close to 11 years, almost half of the considered LT.

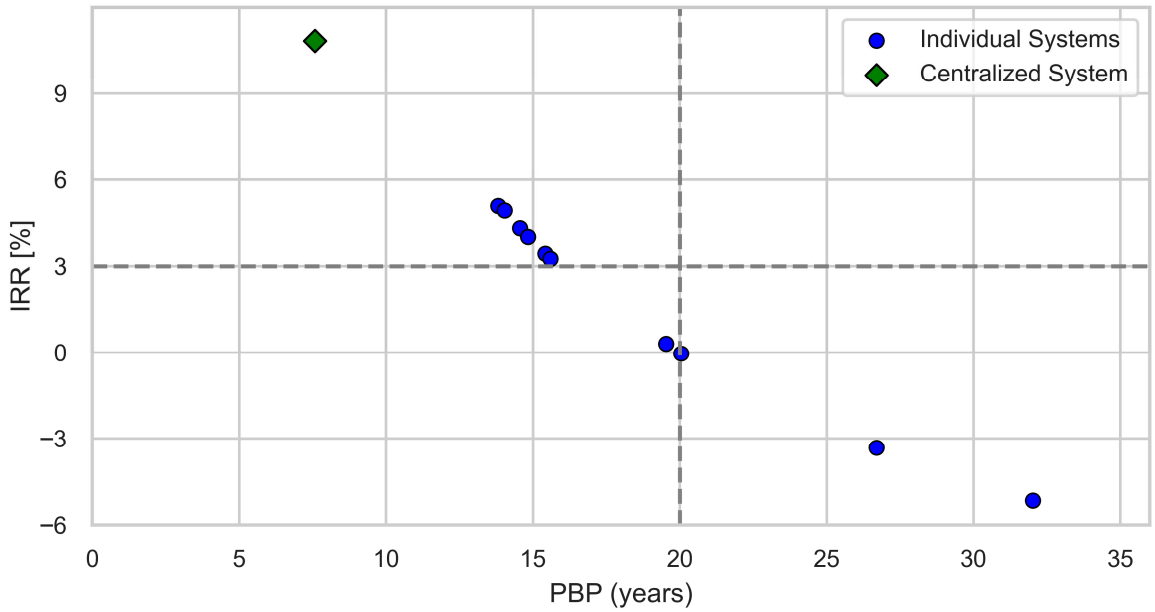


Figure 21. Economic viability comparison between individual and centralized sizing based on IRR versus PBP. Dashed thresholds indicate the viability criteria ($IRR \geq r$ and $PBP \leq LT$). Markers represent each individual prosumer system and the centralized configuration, highlighting cases that fail one or both criteria.

Aggregation also led to a 24.1% reduction in energy-unit cost, reaching a competitive $LCOE$ of €77.98/MWh, compared to an average of €138.08/MWh for individual systems. On the profit side, individual systems show LPOE values ranging from −€110.44/MWh to €16.35/MWh, with an average of −€18.52/MWh, while the centralized configuration reaches an energy-unit profit of €43.92 /MWh.

In summary, centralization does not necessarily improve energy indicators in the Miedes de Aragón case compared to individual solutions. However, it delivers stronger economics. While four individual systems resulted non-viable, collective sizing reduced costs by 42%, resulting in a viable system with competitive $LCOE$. An individual finance assessment shows that aggregation benefits primarily low-demand consumers, improving profitability and lowering energy cost.

5. Discussion on the Initial Data Used to Size Self-Consumption PV Systems

When sizing a self-consumption system, a degree of uncertainty must be assumed in the results, which will depend, among other factors, on the reliability of the initial data. If real hourly data is used, it is assumed that meteorological (solar radiation and ambient temperature) and actual electricity consumption data are available and sufficiently representative of the specific case under study. Meteorological data can be obtained from nearby weather stations or from databases compiled over a significant number of years (16 years or more, as is the case with PVGIS). However, access to hourly electricity consumption data is more limited; it is considered personal data, which makes it difficult to

access. Furthermore, electricity distribution companies do not provide access to historical consumption data covering many years. For example, in Spain, the Datadis platform only has historical consumption data for two years.

The sizing model proposed in this article is based on hourly consumption data from a single year. This raises the question of whether a dataset from only one year can be considered representative, and what level of uncertainty should be assumed in the results.

A statistical study comparing hourly electricity consumption data from two consecutive years has been conducted, using a sample of 118 consumption points as a representative sample. The authors have had access to the electricity consumption data of consumers located in the Calatayud region in northern Spain between 2023 and 2024, where the aforementioned REC operates. Aggregating these 118 electricity consumption figures provides useful information about seasonal consumption patterns. Figure 22 shows the normalized monthly distribution of aggregate electricity consumption. Although the distribution appears fairly uniform, two peaks in consumption can be seen, one in the summer and one in the winter. Figure 23 is a heat map showing that these peaks occur between 1 p.m. and 6 p.m. in July and August, and between 9 a.m. and 12 p.m. in December and January. This pattern is particularly relevant from a self-consumption perspective, as a substantial share of demand is concentrated during daylight hours, especially in summer, when solar availability is higher. In this sense, the aggregated consumption profile suggests favorable conditions for the temporal coincidence between electricity demand and PV generation.

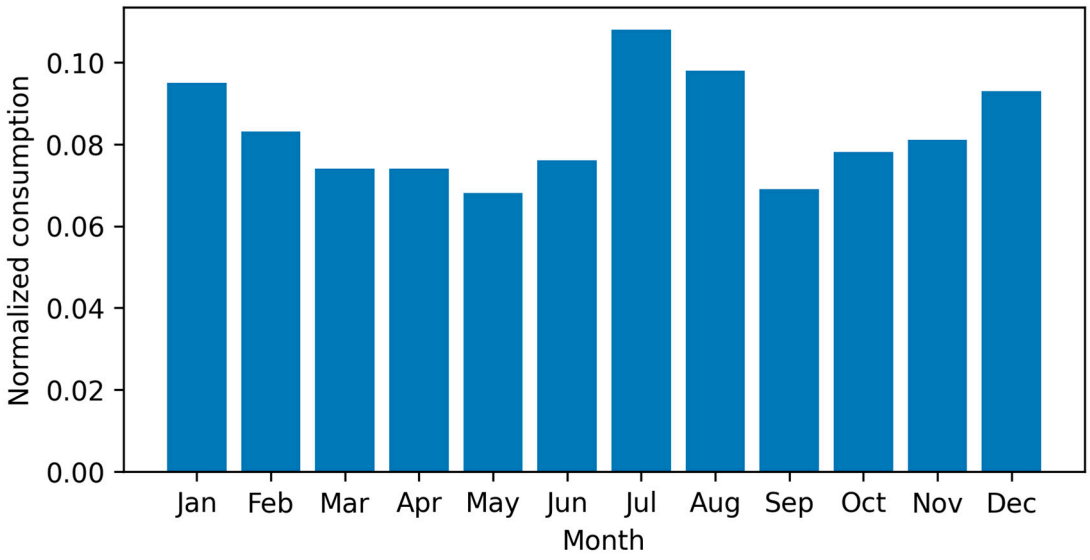


Figure 22. Normalized average monthly electricity consumption for the aggregate of 118 residential consumers in the Calatayud region (Spain). The data covers the period from March 2023 to February 2025 and shows slightly higher consumption levels in summer and winter months.

The statistical study has been carried out obtaining the following indicators:

- Linear regression for each electricity consumption point, comparing the cumulative hourly electricity consumption for 2023 (x-axis) with that for 2024 (y-axis). For each regression, the equation of the line, its slope (m) and the coefficient of determination R^2 are obtained. Values of m and R^2 close to 1 indicate a high degree of equality between the two energy consumption distributions.
- Statistical analysis comparing average annual electricity consumption and its dispersion using the coefficient of variation (CV).
- Statistical analysis comparing hourly means distributions between 2023 and 2024, obtaining the following indicators (expressed in Equations (23) and (24)):

- Pearson correlation coefficient (r): measures the strength and direction of the linear relationship between both variables. Close to 1 $|r|$-values means there is a strong, positive linear relationship.
- Mean absolute percentage error ($MAPE$): measures a forecasting model's accuracy by calculating the average percentage difference between 2023 and 2024 energy values and 2023 values, expressed as a percentage.

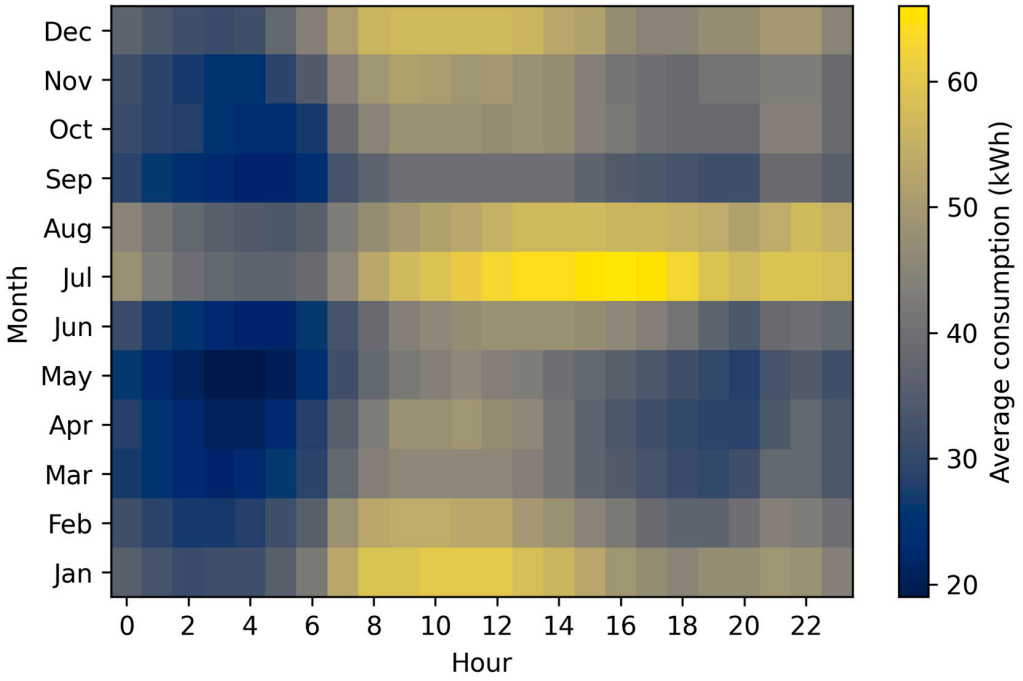


Figure 23. Heat map of average hourly consumption for each month of the year, based on an aggregation of 118 residential consumption profiles from the Calatayud region in Spain. Higher consumption levels are concentrated between 1 p.m. and 6 p.m. in July and August, and between 9 a.m. and 12 p.m. in December and January, indicating that an important share of demand occurs during daylight hours.

$$r = \frac{cov(E_{i,2023}, E_{i,2024})}{\sigma(E_{i,2023})\sigma(E_{i,2024})} \tag{23}$$

$$MAPE = \frac{1}{n}\sum_{i=1}^{n}\left|\frac{E_{i,2023} - E_{i,2024}}{E_{i,2023}}\right| \cdot 100 \tag{24}$$

where i represents temporal unit (n = 24 h); $E_{i,2023}$ and $E_{i,2024}$ are energy values in 2023 and 2024, respectively; and cov and σ indicate covariance and standard deviation.

These statistical results can be used to establish criteria for interpreting the degree of similarity between electricity consumption distributions. We propose the following thresholds:

- $r > 0.95$ and $MAPE < 10\%$ means that distributions are very similar and any one can be used as a representative time pattern.
- $r > 0.90$ and $MAPE < 15\%$ means that distributions have an acceptable similarity, but some uncertainty exists.
- $r < 0.90$ or $MAPE > 15\%$ indicates that the distributions are not similar enough to be considered acceptable.

In addition, $MAPE$ can be used to estimate future prediction uncertainty.

Note that the interest in comparing the distributions of average hourly electricity consumption between different years stems from the fact that average hourly profiles are useful for characterizing consumers' electricity consumption.

The results of the statistical study are shown below:

A linear regression has been performed between cumulative consumption in 2023 (x-axis) and cumulative consumption in 2024 (y-axis), both ordered chronologically, for each of the consumption points.

Figure 24 illustrates a representative regression line for one of the 118 consumers. For this representative case, the fitted line exhibits a slope of m = 1.095 and $R^2 = 0.988$, indicating a high degree of similarity between the two electricity consumption distributions.

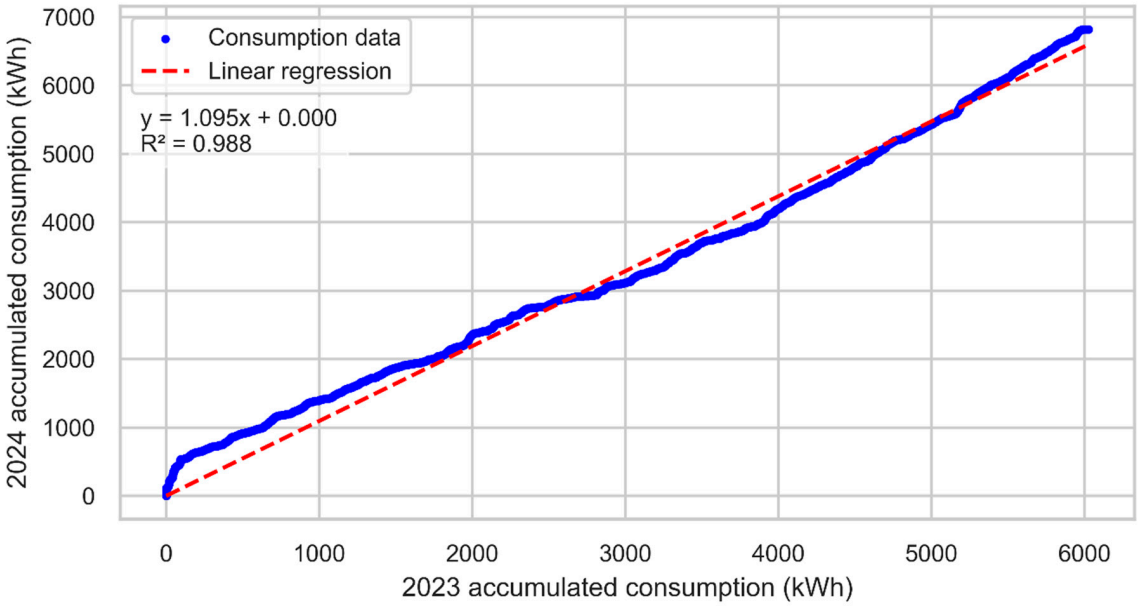


Figure 24. Example linear regression comparing cumulative hourly electricity consumption in 2023 (x-axis) and 2024 (y-axis) for a representative consumer of Calatayud region. The fitted slope and R^2 illustrate interannual similarity in cumulative consumption patterns.

Figure 25 illustrates the outcomes of applying regression analysis to 118 consumption points. The box-plots illustrate the distribution of regression line slope coefficients (m) and R^2-values. The m-values are concentrated very close to 1, suggesting stable behavior from one year to the next. An average slope (m) of 0.999 indicates almost identical average consumption distributions between the two years, and an average R^2-value of 0.997 confirms strong linear correlations across the entire sample.

Table 6 summarizes the main annual consumption statistics for 2023 and 2024. The average annual consumption per consumer increased slightly from 5526 kWh in 2023 to 5626 kWh in 2024 (+1.8%). The annual coefficient of variation (CV) of energy consumption decreased from 334% to 294%, indicating a reduction in consumption dispersion of 12%. However, the mean hourly CV remained stable with a variation of 2% between 2023 and 2024. (~110%), confirming the consistency of intraday variability of demand across both years.

The statistical analysis comparing hourly means electricity consumption distributions between 2023 and 2024 is performed since hourly profiles are useful to characterize the electricity consumption of a consumer. Figure 26 shows the hourly means distributions for 2023 and 2024 for the aforementioned consumer, whose statistical parameter results are as follows:

- Pearson correlation coefficient r = 0.9715.
- Mean absolute percentage error $MAPE$ = 8.91%.

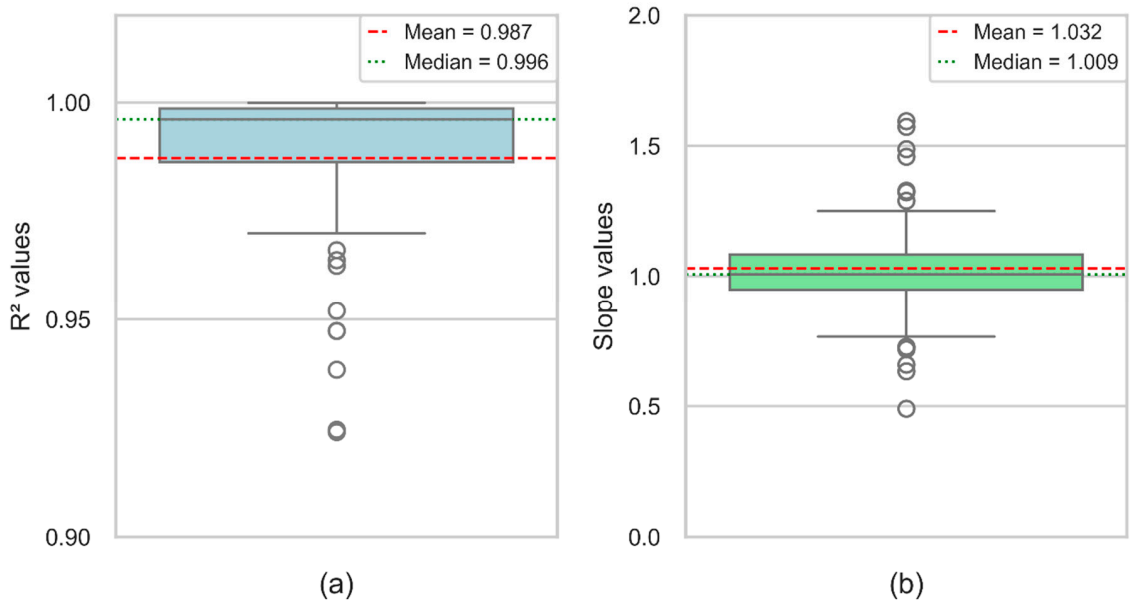


Figure 25. Boxplot distribution of linear regression parameters across 118 supply points (2023 vs. 2024): (**a**) coefficient of determination (R^2) and (**b**) slope m. Circles indicate outlier values. Concentration of m near 1 and high R^2 values indicate strong interannual consistency of cumulative consumption.

Table 6. Comparative annual consumption statistics for 2023 and 2024 based on 118 consumers.

	2023	**2024**	**|Δ| (%)**
Average annual consumption (kWh)	5526	5626	1.8%
CV (annual consumption)	334%	294%	12%
Mean hourly *CV*	110%	113%	2%

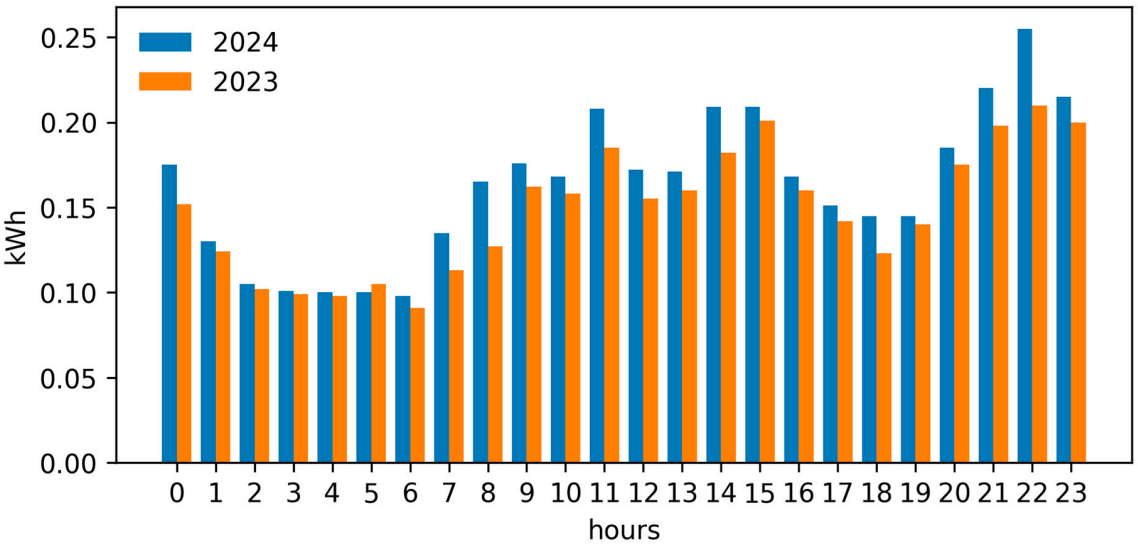


Figure 26. Hour-of-day mean electricity consumption profiles for 2023 and 2024 for a representative consumer of Calatayud region, used to assess similarity of intraday patterns across years. The comparison supports evaluation of the representativeness of one-year hourly data for sizing.

Both the statistical results and the electricity consumption distributions shown in Figure 26 indicate a high degree of similarity between 2023 and 2024 energy consumption distributions. $r > 0.95$ and $MAPE < 0.15$ suggest that either of the two distributions can be used as representative data in this case study.

When applying this statistical analysis to the 118 electricity consumption points, results are expressed in Table 7:

Table 7. Results of the statistical analysis to the 118 electricity consumption points.

	r	***MAPE***
μ	0.90551	17%
σ	0.16438	18%
Q_1	0.92106	7%
Q_3	0.97976	20%

The analysis shows that 75% of the samples have *r*-values up to 0.921 (given by the first quartile Q_1) and 75% have *MAPE*-values lower than 20% (third quartile Q_3). The mean (μ) values of *r* and *MAPE* also confirm the high degree of similarity between the distributions. The low standard deviation (σ) values express their low dispersion. Furthermore, 46% of the samples have $r > 0.95$ and $MAPE < 15\%$, indicating a high degree of similarity. Conversely, 71% of samples have $r > 0.90$ and $MAPE < 25\%$, representing relatively similar hourly consumption profiles with some uncertainty.

This comparative analysis of the hourly electricity consumption of 118 residential consumers in 2023 and 2024 concludes that, in this case study, a single year of data can be considered representative when used as input for sizing PV systems for self-consumption. The analysis indicates an uncertainty of between 10% and 15% in the average hourly electricity consumption values. This conclusion is reinforced by the linear regression results for the consumption distributions in 2023 and 2024, as well as the low differences between the statistical metrics for both years.

It should be noted that the two chosen periods coincide with typical years in which there have been no exceptional climatic, economic or social events, unlike previous years affected by the likes of the 2020 pandemic or the start of the war in Ukraine, which impacted energy consumption habits and costs.

However, it should be noted that these results cannot be generalized, as they relate to electricity consumption in a specific geographical region over a period of only two years. Therefore, it is recommended that the available hourly consumption data be studied over the longest possible period whenever possible.

6. Conclusions

This article presents a newly developed open-source tool to assess and size photovoltaic (PV) self-consumption systems with or without storage (ST) through the evaluation of technical, temporal mismatch, and economic performance parameters. The tool relies on hourly consumption, meteorological, and electricity tariff data over one year, allowing the analysis to approach real operating conditions. The methodology is based on hourly energy-balance simulations considering different system configurations to evaluate how system size interferes with performance.

The work introduces the Mismatch Index (*MI*), derived from the Gini Coefficient, which offers a new perspective on evaluating the alignment between energy consumption patterns and PV system energy output (*SEO*). By comparing the relative temporal distribution of *SEO* and demand, the indicator provides a visual and quantitative understanding of how temporally aligned both distributions are over the analyzed period. When combined with traditional metrics like self-consumption (*SC*) and self-sufficiency (*SS*), it offers a multidimensional perspective that supports the design and assessment of energy systems under different temporal, demand, production, and economic conditions.

A unified tool was presented to support the analysis and sizing of PV self-consumption systems with storage through an integrated technical, temporal, and economic assessment framework. Rather than operating as a mathematical optimization model, the tool is conceived as a transparent decision-support framework based on the sequential evaluation of candidate configurations under self-consumption conditions. Four individual applications compose the tool:

- The Energy Flow (EFA) application evaluates *SC* and *SS* levels under varying PV-ST configurations. It shows system configurations that maximize local PV-ST energy use and grid independence without oversizing or incurring unnecessary cost. When applied to a target, the tool points to different combinations that obtain similar operational performance, allowing the user to select the one that meets their needs and restraints.
- The Consumption–Generation Alignment (CGA) application calculates the Mismatch Index (*MI*), which indicates the degree of temporal alignment between a consumer's energy consumption and the energy produced by the PV-ST system. The closer the *MI* is to zero, the lower the temporal mismatch and the greater the similarity between the relative distributions of demand and system energy output over the analyzed period.
- The Economic Assessment Application (EAA) evaluates the economic performance for different PV-ST configurations based on four main metrics: payback period (*PBP*), internal rate of return (*IRR*), energy-unit cost (*LCOE*) and profitability (*LPOE*). Its visual output illustrates how system size affects long-term economic performance based on real consumption and electricity market prices, allowing the user to identify advantageous configurations that meet their needs and ensure economic viability and profitability.
- The System Sizing Application (SSA) evaluates PV-ST systems through an iterative process and selects one configuration that minimizes temporal mismatch between energy consumption and *SEO*, identifies a technically sufficient configuration based on the stabilization of *SC* and *SS*, and ensures economic viability based on *PBP* and *IRR* constraints, operating as a rule-based decision procedure rather than as a mathematical optimization model.

Together, these applications support consistent evaluation of energy autonomy, temporal alignment between energy consumption and production, and economic performance, offering a structured path for users to understand how system size influences overall behavior and viability, while avoiding unnecessary oversizing once gains become marginal.

When applied to a case study of a residential consumer in Spain, the tool shows how energy consumption and electricity tariffs can guide decision-making toward balanced and viable PV configurations, providing technically robust and economically consistent outcomes.

This case study, based on actual hourly consumption data and meteorological series from a Typical Meteorological Year (TMY) over a full year, resulted in a PV-ST configuration that minimized temporal mismatch (MI_{Daily} of 0.30), improved performance through *SC* and *SS* (0.87 and 0.66, respectively), and ensured long-term economic viability (*PBP* of 14 years, lower than the 20-year lifetime, and *IRR* of 4.92%, higher than the 3% discount rate considered), while obtaining a competitive *LCOE* of €102.78/MWh in comparison to the average electricity market tariff in the consumption period (€138/MWh). These results show that the proposed tool meets its intended purpose by identifying a PV–ST configuration that does not rely on a single performance dimension, but instead balances temporal alignment, energy autonomy, and long-term economic viability. In other words, the selected configuration did not simply reduce grid purchases; it also identified a PV–ST sizing point at which *SC* and *SS* had already stabilized while maintaining stronger temporal

alignment with household demand, which reinforces the practical value of the proposed sizing approach and supports more efficient local use of PV generation.

When applied to an energy community comprising ten individual consumers in Miedes de Aragon (Spain), the tool enables not only the comparison of alternative system configurations, but also the assessment of the technical and economic implications of adopting ten individual systems for each prosumer or a single centralized system. In this case study, the tool indicates that the technical results for the centralized system are moderately superior to those for the individual systems. For instance, the centralized system achieves *SC* and *SS* rates of 0.91 and 0.74, respectively, whereas the individual systems achieve average rates of *SC* = 0.88 and *SS* = 0.73.

However, the economic results show significant differences between the individual and centralized systems. Aggregation reduces CAPEX by 42% (from €39k to €22k). Consequently, the payback period (*PBP*) decreases from a maximum of 32 years for individual systems to 11 years for the centralized system; the net present value (NPV) increases from €1.37k to €20.06k; the internal rate of return (*IRR*) increases from a minimum of 5.16% to a positive value of 10.84%; the levelized cost of electricity (*LCOE*) decreases from €102.78/MWh to €77.98/MWh; and the levelized price of electricity (*LPOE*) increases from −€110.44/MWh to €43.92/MWh.

These results show that the tool can be used not only to support sizing decisions, but also to evaluate how aggregation and system centralization affect the overall technical performance and, above all, the economic viability of collective self-consumption schemes. From the users' perspective, these differences translate into more affordable investment requirements, shorter payback times, lower lifetime electricity costs, and positive economic returns that would not be achieved under the individual-system approach. In this sense, the tool makes the benefits of aggregation directly readable for decision-makers and community members by showing that the main advantage of centralization in this case is not only a moderate improvement in *SC* and *SS*, but a much stronger enhancement in the financial attractiveness and feasibility of the project.

Overall, the proposed methodology and tool provide a basis for decision-making in PV self-consumption system size, bridging technical consistency, temporal alignment, and economic viability. The approach addresses a gap in PV–ST sizing tools by integrating temporal alignment into the sizing process, moving beyond conventional approaches based only on annual balances or economic optimization. The two application contexts (residential and energy community) illustrate its adaptability to individual and aggregated scenarios, as well as robustness across different consumption patterns and scales, and a transparent framework to interpret the relationship between technical performance, temporal behavior, and economic outcomes. In this way, the methodology supports not only the identification of feasible system configurations, but also a more comprehensive understanding of how these different performance dimensions interact under self-consumption conditions while helping avoid unnecessary surplus and oversizing.

Finally, a comparative statistical analysis of hourly electricity consumption has been conducted for 118 residential consumers for two different years, using actual data. The aim of this analysis is to determine the degree of uncertainty when using one-year hourly consumption data as input for PV self-consumption sizing. The study concludes that a single year of data can be considered representative for this purpose. The analysis indicates an uncertainty of between 10% and 15% in the average hourly electricity consumption values. This conclusion is reinforced by a linear regression assessment of the electricity consumption distribution in 2023 and 2024. Linear regressions show slopes (m) and coefficients of determination R^2 close to 1, suggesting a high degree of similarity between the two distributions.

Despite these contributions, this study has some limitations that should be acknowledged. First, the residential case study is based on one year of hourly consumption data, and the representativeness analysis compares only two consecutive years and a geographically restricted sample from the Calatayud region; therefore, the conclusion that one year of data is sufficiently representative should be interpreted cautiously and mainly within the studied context. Second, the economic analysis depends on simplified long-term assumptions, including fixed discount and tariff-growth rates, average PV and storage degradation values, and replacement assumptions, which may not fully capture market volatility or the real aging behavior of batteries and inverters. Finally, the proposed Mismatch Index complements *SC* and *SS* by characterizing the degree of temporal alignment between SEO and electricity demand, but the method does not allow identifying the specific time instant at which the misalignment occurred when the curve is analyzed on its own, and therefore does not fully capture pure time-lag effects between demand and PV supply.

Future work should involve extending the analysis to longer periods of hourly consumption data and to other geographical contexts, as well as investigating possible changes in electricity consumption habits associated with the availability of low-cost electricity at certain times of the day. Future work should also involve incorporating an analysis of systems applied to collective self-consumption, assessing different actors, participation schemes, and benefit-sharing mechanisms to explore how aggregation strategies can enhance equity, efficiency, and overall system performance.

Author Contributions: Conceptualization, K.A.e.S. and L.M.C.; methodology, software, and writing—original draft preparation, K.A.e.S.; validation, formal analysis, investigation, resources, and data curation, K.A.e.S., L.M.C. and R.H.A.; writing—review and editing, K.A.e.S., L.M.C. and R.H.A.; supervision, L.N. and E.L.; project administration, L.M.C.; funding acquisition L.M.C. and L.N. All authors have read and agreed to the published version of the manuscript.

Funding: This work has been possible thanks to the Project LIFE21-CET-ENERCOM-JALON, 101076395, funded by the European Union. Views and opinions expressed are, however, those of the author(s) only and do not necessarily reflect those of the European Union or CINEA. Neither the European Union nor the granting authority can be held responsible for them.

Institutional Review Board Statement: Not applicable.

Informed Consent Statement: Not applicable.

Data Availability Statement: The data presented in this study are available on request from the corresponding author. The data used in this study cannot be made publicly available due to privacy and confidentiality restrictions. The dataset includes real electricity consumption data from individual users, and participant authorization was granted only for the purpose of carrying out system-design and research analyses within the scope of this study. Consent was not provided for public disclosure or broader data sharing. For this reason, the data are not publicly available. They may be made available from the corresponding author only upon reasonable request and subject to the necessary confidentiality and data protection considerations.

Conflicts of Interest: The authors declare no conflicts of interest.

Abbreviations

The following abbreviations are used in this manuscript:

AC	Alternating Current
BMS	Battery Management System
CAPEX	Capital Expenditure
CGA	Consumption–Generation Alignment Application
DC	Direct Current

EFA	Energy Flow Application
EAA	Economic Assessment Application
GC	Gini Coefficient
OPEX	Operating Expenditure
PV	Photovoltaic
PVPC	Voluntary Price for the Small Consumer
SSA	System Sizing Application
ST	Storage

Nomenclature

The following symbols and variables are used in this manuscript:

A	Mismatch Area	-
B	Area under the Lorenz Curve	-
C	Annual operating cost	€
C_{ST}	Storage capacity	kWh
C_{PV}	PV nominal capacity	kWp
CV	Coefficient of Variation	%
d_{PV}	PV degradation rate	%/year
d_{ST}	ST degradation rate	%/year
EE	Export Energy Ratio	-
E^{SC}	Self-consumption energy over the system lifetime	kWh
E^{Export}	Exported energy over the system lifetime	kWh
E_x^y	Energy from origin X to destination Y	kWh
E_{LOAD}	Load demand	kWh
E_{PV}	PV-generated energy	kWh
E_{ST}	ST energy exchange	kWh
$E_{ST,MAX}$	Maximum ST energy capacity	kWh
E_{GRID}	Grid energy exchange	kWh
G	Irradiance	kW/m^2
G^*	Reference solar irradiance	kW/m^2
g_T	Tariff growth rate	%/year
g_C	OPEX growth rate	%/year
I_0	Initial investment	€
IE	Import Energy Ratio	-
IRR	Internal Rate of Return	%
$LCOE$	Levelized Cost of Energy	€/MWh
$LPOE$	Levelized Profit of Energy	€/MWh
LT	PV-ST system lifetime period	year
$M(t)$	Instantaneous Self-Consumption Power	kW
MI	Mismatch Index	-
NPV	Net Present Value	€
$NOCT$	Nominal Operating Cell Temperature	°C
n_y	Number of Days in the Year	-
PBP	Payback Period	year
P_{PV}^*	PV nominal power	kW
P_{PV}	PV-generated power	kW
P_{Load}	Load power demand	kW
P_{ST}	ST power exchange	kW
P_{Grid}	Power exchanged with the grid	kW
r	Discount rate	%
REV	Economic revenues	€
SC	Self-Consumption Ratio	-

SS	Self-Sufficiency Ratio	-
SOC	State of Charge of the battery	%
SEO	System Energy Output	kWh
T_a	Ambient temperature	°C
T_c	PV cell temperature	°C
t	Time	hour or year
γ	Power temperature coefficient	%/°C
η	System efficiency	%
τ	Stabilization Tolerance Criterion	-
ρ	Mismatch Tolerance	-
R^2	Coefficient of Determination	-

Appendix A

Table A1. Comparative overview of 36 PV self-consumption sizing tools based on temporal resolution, coincidence criterion, and access. Tool access and availability were verified by the authors using publicly available official sources at the time of revision.

Tool	Scope	Method	Data Resolution	Temporal Coincidence Criterion Used for Sizing?	Access
Evans & Facinelli	Off-grid (stand-alone PV)	Technical model/simulation sweep	Aggregated (monthly/annual)	No	Research
RAPSIM	Hybrid microgrid	Simulation and optimal sizing	Hourly (profiles)	No	Free (open-source)
CPF (Clean Power tFinance)	On-grid	Web design (technical and financial)	Unspecified	No	Discontinued
Hybrid2	Hybrid	Probabilistic optimization and simulation	Hourly (TMY/profiles)	No	Discontinued
PVOptimize	On-grid	Simulation and economic rule	Unspecified	No	Limited (region-specific)
PVToolbox (MATLAB)	Hybrid/PV performance	Simulation (MATLAB/Simulink)	Unspecified	No	Research
SIPM	General PV performance model	Technical inverter model	N/A (model)	No	Research
SPAPM	General PV performance model	Technical PV array model	N/A (model)	No	Research
Five-parameter array performance model	General PV performance model	Technical PV array model	N/A (model)	No	Research
HySim	Hybrid	Simulation and optimization	Unspecified	No	Research
PVForm	General PV/on-grid	Simulation sweep	Unspecified	No	Research
PVSS	General PV/on-grid	Technical simulation	Unspecified	No	Research
REPS.OM	On-grid/off-grid/hybrid	Discrete-sampling optimization	Unspecified	No	Research
SOLCEL	Off-grid/on-grid/hybrid	Simulation sweep and basic economics	Unspecified	No	Research
SOLSTOR	Hybrid	Optimization (LCC)	Unspecified	No	Research
UW-hybrid (TRNSYS)	Hybrid	Simulation	Unspecified	No	Research
Dymola/Modelica	Hybrid	Object-oriented modelling	Unspecified	No	Paid
HOMER	Off-grid/on-grid/hybrid	Optimization (enumeration) and hourly simulation	Hourly	No	Paid

Table A1. *Cont.*

Tool	Scope	Method	Data Resolution	Temporal Coincidence Criterion Used for Sizing?	Access
OnGrid	On-grid	Simulation and incentives	Unspecified	No	Paid
Polysun	PV/PVT/solar cooling	Simulation sweep	Unspecified	No	Paid
PV DesignPro-G/PV-DesignPro	On-grid	Hourly simulation and finance	Hourly	No	Paid
PV F-Chart	Off-grid/on-grid	Simplified method	Monthly (averages)	No	Paid
PV*SOL Expert	On-grid	3d/shading simulation sweep	Unspecified	No	Paid
PVsyst	On-grid/off-grid	Simulation (parametric)	Sub-hourly/hourly	No	Paid
SolarDesignTool	On-grid	Layout/design and simulation	Unspecified	No	Paid
SolarPro	On-grid	Layout/design and simulation	Unspecified	No	Paid
SolarPro (CPE—Clean Power Estimator)	On-grid	Web feasibility	Aggregated	No	Paid
TRNSYS/UW-Hybrid	Hybrid	Dynamic simulation	Hourly/sub-hourly	No	Paid
HySys	Hybrid (off-grid)	Simulation (matlab) and lcc	Unspecified	No	Research
IPSYS	Hybrid multi-source	Simulation/optimization	Unspecified	No	Research
INSEL	General PV platform	Block-based simulation	Unspecified	No	Free
PVSIM	On-grid/off-grid	Simulation sweep	Unspecified	No	Free
PVWatts	On-grid	Simplified simulation	Monthly/annual	No	Free
SAM (NREL)	On-grid/off-grid	Simulation and finance	Hourly	No	Free
iHOGA	Hybrid	Multi-objective ga optimization	Unspecified	No	Free (limited version)
RETScreen	General PV	Economic feasibility	Aggregated	No	Free (limited version)

References

1. European Commission. *Clean Energy for All Europeans Package, Energy, Climate Change, Environment*; European Commission: Luxembourg, 2019. Available online: https://eur-lex.europa.eu/legal-content/EN/TXT/HTML/?uri=CELEX:52016DC0860 (accessed on 29 January 2024).
2. SolarPower Europe. New Analysis Reveals that EU Solar Stalls, 2025 Projected to Mark First Year of Market Decline in a Decade. Available online: https://www.solarpowereurope.org/press-releases/new-analysis-reveals-that-eu-solar-stalls-2025-projected-to-mark-first-year-of-market-decline-in-a-decade (accessed on 20 October 2025).
3. Statista. Residential Solar Photovoltaics in Europe—Statistics & Facts. Available online: https://www.statista.com/topics/13626/residential-solar-photovoltaics-in-europe/?srsltid=AfmBOor7uqVX4wWkDK5fatn2Vc4dhUq1k3q_nFPRw4jjpN7ke8A7G_rf (accessed on 11 November 2025).
4. EUPD Group. EUPD Research Reveals Top European Residential Solar Markets and Most Impacting Installers Amidst Booming Market Growth. Available online: https://eupd-group.com/eupd-research-reveals-top-european-residential-solar-markets-and-most-impacting-installers-amidst-booming-market-growth/ (accessed on 21 July 2025).
5. Luthander, R.; Widén, J.; Nilsson, D.; Palm, J. Photovoltaic self-consumption in buildings: A review. *Appl. Energy* **2015**, *142*, 80–94. [CrossRef]
6. Castaneda, M.; Zapata, S.; Cherni, J.; Aristizabal, A.J.; Dyner, I. The long-term effects of cautious feed-in tariff reductions on photovoltaic generation in the UK residential sector. *Renew. Energy* **2020**, *155*, 1432–1443. [CrossRef]
7. Ciocia, A.; Amato, A.; Di Leo, P.; Fichera, S.; Malgaroli, G.; Spertino, F.; Tzanova, S. Self-Consumption and Self-Sufficiency in Photovoltaic Systems: Effect of Grid Limitation and Storage Installation. *Energies* **2021**, *14*, 1591. [CrossRef]

8. Li, J.; Danzer, M.A. Optimal charge control strategies for stationary photovoltaic battery systems. *J. Power Sources* **2014**, *258*, 365–373. [CrossRef]
9. Perpiñan, O.; Lorenzo, E.; Castro, M.A. On the calculation of energy produced by a PV grid-connected system. *Prog. Photovolt. Res. Appl.* **2007**, *15*, 265–274. [CrossRef]
10. Muñoz-Rodríguez, F.J.; Jiménez-Castillo, G.; de la Casa Hernández, J.; Aguilar Peña, J.D. A new tool to analysing photovoltaic self-consumption systems with batteries. *Renew. Energy* **2021**, *168*, 1327–1343. [CrossRef]
11. Tushar, Q.; Zhang, G.; Giustozzi, F.; Bhuiyan, M.A.; Hou, L.; Navaratnam, S. An integrated financial and environmental evaluation framework to optimize residential photovoltaic solar systems in Australia from recession uncertainties. *J. Environ. Manag.* **2023**, *346*, 119002. [CrossRef]
12. Fina, B.; Monsberger, C.; Auer, H. Simulation or estimation?—Two approaches to calculate financial benefits of energy communities. *J. Clean. Prod.* **2022**, *330*, 129733. [CrossRef]
13. Osman, M.G.; Lazaroiu, G.; Hamad, S.A.; Messaoud, H.; Mohammed, D.; Stoica, D. Analysis of Photovoltaic Systems with Battery Storage, Electric Vehicle Charging, and Smart Energy Management. *Sustainability* **2025**, *17*, 3887. [CrossRef]
14. Gini, C. On the measurement of concentration and variability of characters. *Metron—Int. J. Stat.* **2005**, *63*, 1–38.
15. Fellman, J. Estimation of Gini coefficients using Lorenz curves. *J. Stat. Econom. Methods* **2012**, *1*, 31–38. Available online: https://www.researchgate.net/publication/259870644 (accessed on 14 July 2023).
16. Sitthiyot, T.; Holasut, K. A simple method for estimating the Lorenz curve. *Humanit. Soc. Sci. Commun.* **2021**, *8*, 268. [CrossRef]
17. Jacobson, A.; Milman, A.D.; Kammen, D.M. Letting the (energy) Gini out of the bottle: Lorenz curves of cumulative electricity consumption and Gini coefficients as metrics of energy distribution and equity. *Energy Policy* **2005**, *33*, 1825–1832. [CrossRef]
18. Das, A.K. Quantifying photovoltaic power variability using Lorenz curve. *J. Renew. Sustain. Energy* **2014**, *6*, 033124. [CrossRef]
19. Gao, D.; Zhi, Y.; Rong, X.; Yang, X. Mismatch analysis of rooftop photovoltaics supply and farmhouse load: Data dimensionality reduction and explicable load pattern mining via hybrid deep learning. *Appl. Energy* **2025**, *377*, 124520. [CrossRef]
20. Ballesteros-Gallardo, J.A.; Arcos-Vargas, A.; Núñez, F. Optimal design model for a residential PV storage system. An application to the Spanish case. *Sustainability* **2021**, *13*, 575. [CrossRef]
21. Cirone, D.; Bruno, R.; Bevilacqua, P.; Perrella, S.; Arcuri, N. Techno-Economic Analysis of an Energy Community Based on PV and Electric Storage Systems in a Small Mountain Locality of South Italy: A Case Study. *Sustainability* **2022**, *14*, 13877. [CrossRef]
22. Isaac, S.; Shubin, S.; Rabinowitz, G. Cost-Optimal Net Zero Energy Communities. *Sustainability* **2020**, *12*, 2432. [CrossRef]
23. Villar, C.H.; Neves, D.; Silva, C.A. Solar PV self-consumption: An analysis of influencing indicators in the Portuguese context. *Energy Strategy Rev.* **2017**, *18*, 224–234. [CrossRef]
24. Drury, E.; Denholm, P.; Margolis, R. *The Impact of Different Economic Performance Metrics on the Perceived Value of Solar Photovoltaics—NREL/TP-6A20-52197*; National Renewable Energy Laboratory: Golden, CO, USA, 2011. Available online: https://docs.nrel.gov/docs/fy12osti/52197.pdf (accessed on 3 July 2025).
25. Yan, J.; Yang, Y.; Elia Campana, P.; He, J. City-level analysis of subsidy-free solar photovoltaic electricity price, profits and grid parity in China. *Nat. Energy* **2019**, *4*, 709–717. [CrossRef]
26. Kazem, H.A.; Chaichan, M.T.; Al-Waeli, A.H.A.; Gholami, A. A systematic review of solar photovoltaic energy systems design modelling, algorithms, and software. *Energy Sources Part A Recovery Util. Environ. Eff.* **2022**, *44*, 6709–6736. [CrossRef]
27. PVsyst SA. *PVsyst*, Version 8.0; PVsyst SA: Satigny, Switzerland, 2024. Available online: https://www.pvsyst.com/en/products/pvsyst-8/ (accessed on 26 February 2026).
28. HOMER Energy LLC. *HOMER Pro—Microgrid Optimization Software*, Version 3.18.4; HOMER Energy LLC: Boulder, CO, USA, 2024. Available online: https://homerenergy.com/homer-pro (accessed on 26 February 2026).
29. NREL. *SAM 2025.4.16*; National Renewable Energy Laboratory: Golden, CO, USA, 2025. Available online: https://sam.nlr.gov/ (accessed on 26 February 2026).
30. Python 3.14.0. 2025. Available online: https://docs.python.org/3/ (accessed on 20 October 2025).
31. CERCA—Comunidad de Energías Renovables de la Comarca de Calatayud. 2023. Available online: https://cercaenergia.com/ (accessed on 5 May 2025).
32. European Commission. *PVGIS 5.2—The Joint Research Centre: EU Science Hub*; European Commission: Luxembourg. Available online: https://joint-research-centre.ec.europa.eu/photovoltaic-geographical-information-system-pvgis/pvgis-releases/pvgis-52_en (accessed on 24 November 2025).
33. Datadis. Available online: https://datadis.es/home (accessed on 23 October 2025).
34. Carrêlo, I.B.; Almeida, R.H.; Narvarte, L.; Martinez-Moreno, F.; Carrasco, L.M. Comparative analysis of the economic feasibility of five large-power photovoltaic irrigation systems in the Mediterranean region. *Renew. Energy* **2020**, *145*, 2671–2682. [CrossRef]
35. Silva, K.A.; Carrasco, L.M.; Mata, A.L. Energy Flow Algorithm to the optimization of on-grid PV buildings with or without backup storage. In Proceedings of the EU PVSEC 2023, Lisboa, Portugal, 18–22 September 2023. [CrossRef]
36. Gergely, L.Z.; Csoknyai, T.; Horváth, M. Novel load matching indicators for photovoltaic system sizing and evaluation. *Appl. Energy* **2022**, *327*, 120123. [CrossRef]

37. Salom, J.; Marszal, A.J.; Widén, J.; Candanedo, J.; Lindberg, K.B. Analysis of load match and grid interaction indicators in net zero energy buildings with simulated and monitored data. *Appl. Energy* **2014**, *136*, 119–131. [CrossRef]
38. Ofry, E.; Braunstein, A. The loss of power supply probability as a technique for designing stand-alone solar electrical (photovoltaic) systems. *IEEE Trans. Power Appar. Syst.* **1983**, *PAS-102*, 1171–1175. [CrossRef]
39. Yang, H.; Zhou, W.; Lu, L.; Fang, Z. Optimal sizing method for stand-alone hybrid solar–wind system with LPSP technology by using genetic algorithm. *Sol. Energy* **2008**, *82*, 354–367. [CrossRef]
40. Egido, M.; Lorenzo, E. The sizing of stand alone PV-system: A review and a proposed new method. *Sol. Energy Mater. Sol. Cells* **1992**, *26*, 51–69. [CrossRef]
41. Shell International B.V. Shell Sky Scenario: A Scenario for Meeting the Goals of the Paris Agreement. 2018. Available online: https://www.ourenergypolicy.org/wp-content/uploads/2018/03/shell-scenarios-sky-1.pdf (accessed on 5 March 2026).
42. Bielewski, M.; Pfrang, A.; Bobba, S.; Kronberga, A.; Georgakaki, A.; Letout, S.; Kuokkanen, A.; Mountraki, A.; Ince, E.; Shtjefni, D.; et al. *Clean Energy Technology Observatory: Batteries for Energy Storage in the European Union—2022 Status Report on Technology Development, Trends, Value Chains and Markets*; European Commission: Luxembourg, 2022. [CrossRef]
43. Universidad Politécnica de Madrid. SISIFO: An Online Simulator of PV Systems. Available online: https://www.sisifo.info/es/default (accessed on 31 July 2023).
44. Precio Voluntario para el Pequeño Consumidor (PVPC). Available online: https://www.miteco.gob.es/es/energia/energia-electrica/electricidad/contratacion-suministro/precio-voluntario.html (accessed on 7 July 2025).
45. Análisis | ESIOS Electricidad · Datos · Transparencia. Available online: https://www.esios.ree.es/es/analisis/1739 (accessed on 5 December 2024).
46. Fraunhofer ISE. *Photovoltaics Report, Freiburg*; Fraunhofer ISE: Freiburg, Germany, 2025. Available online: www.ise.fraunhofer.de (accessed on 3 February 2026).
47. Interest Rates, Government Securities, Treasury Bills for Spain (INTGSTESM193N) | FRED | St. Louis Fed. Available online: https://fred.stlouisfed.org/series/INTGSTESM193N# (accessed on 1 October 2025).
48. Home | Informes del Sistema. Available online: https://www.sistemaelectrico-ree.es/es (accessed on 3 October 2025).
49. Photovoltaic Lifetime Project | Photovoltaic Research | NREL. Available online: https://www.nrel.gov/pv/lifetime (accessed on 1 October 2025).
50. Shimura, S.; Herrero, R.; Zuffo, M.K.; Baesso Grimoni, J.A. Production costs estimation in photovoltaic power plants using reliability. *Sol. Energy* **2016**, *133*, 294–304. [CrossRef]
51. The Economics of Utility-Scale Solar Generation: Summary. Available online: https://www.ref.org.uk/ref-blog/374-the-economics-of-utility-scale-solar-generation-summary (accessed on 1 October 2025).
52. Alotaibi, M.A.; Eltamaly, A.M. A Smart Strategy for Sizing of Hybrid Renewable Energy System to Supply Remote Loads in Saudi Arabia. *Energies* **2021**, *14*, 7069. [CrossRef]
53. Eltamaly, A.M. A novel energy storage and demand side management for entire green smart grid system for NEOM city in Saudi Arabia. *Energy Storage* **2024**, *6*, e515. [CrossRef]
54. Ketjoy, N.; Mensin, Y.; Mensin, P.; Kaewpanha, M.; Khakhu, S.; Chantarapongphan, C.; Sulaiman, S.I. Development of a Degradation Model for Lifespan Prediction: A Case Study on Grid-Scale Battery Energy Storage Systems in Thailand. *Batteries* **2025**, *11*, 429. [CrossRef]
55. Normativa de Autoconsumo | Idae. Available online: https://www.idae.es/tecnologias/energias-renovables/oficina-de-autoconsumo/normativa-de-autoconsumo (accessed on 1 October 2025).

Disclaimer/Publisher's Note: The statements, opinions and data contained in all publications are solely those of the individual author(s) and contributor(s) and not of MDPI and/or the editor(s). MDPI and/or the editor(s) disclaim responsibility for any injury to people or property resulting from any ideas, methods, instructions or products referred to in the content.